

Phosphorus–Nitrogen Compounds. 18. Syntheses, Stereogenic Properties, Structural and Electrochemical Investigations, Biological Activities, and DNA Interactions of New Spirocyclic Mono- and Bisferrocenyldiphosphazene Derivatives

Nuran Asmafiliz,[†] Zeynel Kılıç,^{*,†} Aslı Öztürk,[‡] Tuncer Hökelek,[‡] L. Yasemin Koç,[§] Leyla Açık,^{||} Özgül Kısa,[⊥] Ali Albay,[⊥] Zafer Üstündağ,^{||} and Ali Osman Solak[†]

[†]Department of Chemistry, Ankara University, 06100 Ankara, Turkey, [‡]Department of Physics, Hacettepe University, 06800 Ankara, Turkey, [§]Department of Biology, Ankara University, 06100 Ankara, Turkey, ^{||}Department of Biology, Gazi University, 06500 Ankara, Turkey, [⊥]Department of Medical Microbiology, Gülhane Military Medical Academy and Medical Faculty, 06018 Ankara, Turkey, and ^{||}Department of Chemistry, Dumlupınar University, Kütahya, Turkey

Received May 29, 2009

The reactions of hexachlorocyclotriphosphazatriene, $N_3P_3Cl_6$, with mono- (**1** and **2**) and bisferrocenyldiamines (**3–5**), $FcCH_2NH(CH_2)_nNHR_1$ ($R_1 = H$ or $FcCH_2-$), produce mono- (**6** and **7**) and spirocyclic bisferrocenyldiphosphazenes (**8–10**). The fully substituted phosphazenes (**11–15** and **18–21**) are obtained from the reactions of corresponding partly substituted phosphazenes (**6–10**) with excess pyrrolidine and $NH_2(CH_2)_3ONa$, respectively. The reactions of **6** with 1-aza-12-crown-4 afford geminal (**16**) and tris (**17**) crown ether-substituted phosphazenes. The structural investigations of the compounds have been verified by elemental analyses, mass spectrometry, Fourier transform IR, 1H , ^{13}C , and ^{31}P NMR, and DEPT, COSY, HETCOR, and HMBC techniques. The crystal structures of **7**, **10**, **11**, and **15** have been determined by X-ray crystallography. In **16** and **17**, there are one and two stereogenic P atoms, respectively, and they are expected to be in enantiomeric mixtures. The structures of **18–21** look similar to a propeller. In **20** and **21**, there are two stereogenic P atoms, and they exist as cis (meso; **20a** and **21a**) and trans (racemic; **20b** and **21b**) geometric isomers, according to the chiral solvating agent (S)-(+)-2,2,2-trifluoro-1-(9'-anthryl)ethanol experiments. Moreover, the compounds **18** and **19** have three stereogenic P atoms, and they exist as enantiomeric mixtures. Cyclic voltammetric investigations of compounds **6–21a** reveal that ferrocene redox centers undergo oxidation concurrently at the same potential with basically reversible peaks, and these compounds appear to be quite robust electrochemically. The compounds **11–15** have been screened for antibacterial activity against Gram positive and Gram negative bacteria and for antifungal activity against yeast strains. The compounds **11**, **12**, **14**, and **15** are evaluated for antituberculosis activity against reference strain *Mycobacterium tuberculosis* H37Rv (ATCC 27294). Interactions between compounds **11–15** and pBR322 plasmid DNA are studied by agarose gel electrophoresis. These compounds induce conformational changes in the DNA helix.

Introduction

Cyclophosphazene and poly(organo)phosphazene derivatives, which exhibit a variety of different functional groups

and contain alternate P and N atoms in their cyclic and linear backbones, are an important family of inorganic systems.^{1,2} It is well-known that ferrocene and its derivatives are very important compounds for photochemistry^{3–5} and modern

*To whom correspondence should be addressed. E-mail: zkilic@science.ankara.edu.tr.

(1) (a) Chandrasekhar, V.; Thilagar, P.; Pandian, B. M. *Coord. Chem. Rev.* **2007**, 251, 1045–1074. (b) Chandrasekhar, V.; Krishnan, V. *Adv. Inorg. Chem.* **2002**, 53, 159–211. (c) Bertani, R.; Chaux, F.; Gleria, M.; Metrangolo, P.; Milani, R.; Pilati, T.; Resnati, G.; Sansotera, M.; Venzo, A. *Inorg. Chim. Acta* **2007**, 3(360), 1191–1199. (d) Contractor, S. R.; Kılıç, Z.; Shaw, R. A. *J. Chem. Soc., Dalton Trans.* **1987**, 2023–2029. (e) Deutch, W. F.; Hursthouse, M. B.; Kılıç, Z.; Parkers, H. G.; Shaw (nee Gözen), L. S.; Shaw, R. A. *Phosphorus, Sulfur, Silicon* **1987**, 32, 81–85. (f) Rajeswara Rao, M.; Gayatri, G.; Kumar, A.; Narahari Sastry, G.; Ravikanth, M. *Chem. Eur. J.* **2009**, 15, 3488–3496.

(2) (a) Allcock, H. R. *Curr. Opin. Solid State Mater. Sci.* **2006**, 10, 231–240. (b) Allcock H. R. *Chemistry and Applications of Polyphosphazenes*; John Wiley & Sons: New York, 2003. (c) Carriedo, G. A.; Alonso, F. G.; Gonzalez, P. A.; Menendez, J. R. *J. Raman Spectrosc.* **1998**, 29, 327–330. (d) De Jaeger, R.; Gleria, M. *Prog. Polym. Sci.* **1998**, 23, 179–276. (e) Gleria, M.; De Jaeger, R. *Inorg. Organomet. Polym.* **2001**, 11, 1–45.

(3) Fery-Forgues, S.; Delavaux-Nicot, B. *J. Photochem. Photobiol. A* **2000**, 132, 137–159.

(4) Hill, H. A. U.; Page, D. J.; Walton, N. J. *J. Electroanal. Chem.* **1987**, 217, 141–158.

(5) Bozak, R. E. *Adv. Photochem.* **1971**, 8, 227–244.

organometallic chemistry⁶ because of their outstanding stabilities, generating novel materials possessing interesting chemical, electrical, optical, and magnetic properties.^{7,8} A scan of the literature shows that ferrocenylphosphazene derivatives are very limited.^{9,10} The involvement of ferrocene derivatives with the phosphazene ring is also limited to monofunctional reagents for the preparation of electroactive ferrocenylphosphazenes^{6a,9} and dendrimers.¹⁰ To the best of our knowledge, there are no reports on the reactions of ferrocenyldiamines with $N_3P_3Cl_6$ in the literature. Therefore, our study focused primarily on the substitution reactions of $N_3P_3Cl_6$ with ferrocenyldiamines with the aim of preparing electron-rich reservoir complexes capable of acting as electron-transfer mediators.

Phosphazene derivatives are of considerable interest in various areas having technological and medicinal importance,^{2a,b} such as the production of lubricants,¹¹ advanced elastomers,^{2a,12} rechargeable batteries,¹³ anticancer,¹⁴ antibacterial reagents,¹⁵ biomedical materials, and synthetic bones.¹⁶ In addition, biological activities of ferrocenyldiamines (the starting materials used for this study) against

Mycobacterium tuberculosis H37Rv, which infects one-third of the world's population,¹⁷ are known.¹⁸ Recently, the stereogenic properties of cyclophosphazenes were discovered as a new subject of interest.^{19,20} Thus, the investigations of some of the stereogenic phosphazene derivatives have been made by ³¹P NMR spectroscopy upon the addition of chiral solvating agent (CSA)^{19,21,22} and high-performance liquid chromatography techniques.^{23,24}

We report here (i) the synthesis of new spirocyclic mono- (**6** and **7**) and bisferrocenylphosphazenes (**8–10**), (ii) the preparation of tetrapyrrolidinophosphazenes (**11–15**), (iii) the substitutions of Cl atoms of **6** with 1-aza-12-crown-4, which give the bis-crown ether- (**16**) and tris-crown ether-substituted (**17**) phosphazenes, (iv) the synthesis of *cis*- (**18a–21a**) and *trans*-bis(N/O)-substituted products (**18b–21b**) (Scheme 1), (v) the stereogenic properties of **19a**, **19b**, **21a**, and **21b** investigated by ³¹P NMR measurements in the presence of CSA, (vi) the determination of the structures of compounds by elemental analyses, mass spectrometry, Fourier transform (FTIR), one-dimensional (1D) ¹H, ¹³C, and ³¹P NMR, distortionless enhancement by polarization transfer (DEPT), and two-dimensional (2D) correlation spectroscopy (COSY), heteronuclear shift correlation (HETCOR), and heteronuclear multiple-bond correlation (HMBC) techniques, (vii) the solid-state structures of **7**, **10**, **11**, and **15** established by X-ray diffraction techniques, (viii) the electrochemical behavior and structural correlations of ferrocenylphosphazene derivatives, (ix) biological activities of **11**, **12**, **14**, and **15** against *M. tuberculosis* H37Rv reference strain, (x) investigations of antibacterial and antifungal activity of **11–15**, and (xi) interactions between these compounds and pBR322 plasmid DNA examined by agarose gel electrophoresis.^{25,26}

Experimental Section

General Methods. $N_3P_3Cl_6$ (Aldrich), ferrocenecarboxaldehyde (Aldrich), CSA (Aldrich), aliphatic amines (Fluka), pyrrolidine (Fluka), 1-aza-12-crown-4 (Fluka), and 3-amino-1-propanol (Fluka) were purchased and used without further purification. All reactions have been monitored using thin-layer chromatography in different solvents and chromatographed by using silica gel. All experiments were carried out under an argon atmosphere. ¹H, ¹³C, and ³¹P NMR, HETCOR, COSY, and HMBC spectra were recorded on a Bruker DPX FT-NMR (500 MHz) spectrometer (SiMe₄ as internal and 85% H₃PO₄ as external standards). The spectrometer was equipped with a 5 mm PABBO BB inverse-gradient

(6) (a) Chandrasekhar, V.; Andavan, G. T. S.; Nagendran, S.; Krishnan, V.; Azhakar, R.; Butcher, R. J. *Organometallics* **2003**, *22*, 976–986. (b) Cao, R., Jr.; Diaz-Garcia, A. M.; Caob, R. *Coord. Chem. Rev.* **2009**, *253*, 1262–1275.

(7) (a) Astruc, D. *Acc. Chem. Res.* **2000**, *33*, 287–298. (b) Grayson, S. M.; Fréchet, J. M. J. *J. Chem. Rev.* **2001**, *101*, 3819–3868.

(8) Barlow, S.; Bunting, H. E.; Ringham, C.; Green, J. C.; Bublitz, G. U.; Boxer, S. G.; Perry, J. W.; Marder, S. R. *J. Am. Chem. Soc.* **1999**, *121*, 3715–3723.

(9) (a) Muralidharan, K.; Reddy, N. D.; Elias, A. J. *Inorg. Chem.* **2000**, *39*, 3988–3994. (b) Nataro, C.; Myer, C. N.; Cleaver, W. M.; Allen, C. W. *J. Organomet. Chem.* **2001**, *637–639*, 284–290. (c) Myer, C. M.; Allen, C. W. *Inorg. Chem.* **2002**, *41*, 60–66. (d) Sengupta, S. *Polyhedron* **2003**, *22*, 1237–1240. (e) Muralidharan, K.; Elias, A. J. *Inorg. Chem.* **2003**, *42*, 7535–7543. (f) Elias, A. J.; Muralidharan, K.; Kumar, M. S.; Venugopalan, P. *J. Fluorine Chem.* **2006**, *127*, 1046–1053.

(10) (a) Sengupta, S. *Tetrahedron Lett.* **2003**, *44*, 7281–7284. (b) Schneider, R.; Köllner, C.; Weber, I.; Togni, A. *Chem. Commun.* **1999**, 2415–2416.

(11) Zhu, J.; Liu, W.; Chu, R.; Meng, X. *Tribology Int.* **2007**, *40*(1), 10–14.

(12) Allcock, H. R.; Napierala, M. E.; Cameron, C. G.; O'Connor, S. J. *Macromolecules* **1996**, *29*, 1951–1956.

(13) (a) Xu, G.; Lu, Q.; Yu, B.; Wen, L. *Solid State Ionics* **2006**, *177*, 305–309. (b) Morford, R. V.; Kellam, E. C.; Hofmann, M. A.; Baldwin, R.; Allcock, H. R. *Solid State Ionics* **2000**, *133*, 171–1777. (c) Allcock, H. R.; Kellam, E. C.; Morford, R. V.; Conner, D. A.; Welna, D. T.; Chang, Y.; Allcock, H. R. *Macromolecules* **2007**, *40*, 322–328. (d) Klein, R.; Welna, D. T.; Weikel, A.; Allcock, H. R.; Runt, J. *Macromolecules* **2007**, *40*, 3990–3995.

(14) Brandt, K.; Bartczak, T. J.; Kruszynski, R.; Porwolik-Czomperlik, I. *Inorg. Chim. Acta* **2001**, *322*, 138–144.

(15) (a) Yılmaz, Ö.; Aslan, F.; Öztürk, A. İ.; Vanlı, N. S.; Kırbağ, S.; Arslan, M. *Bioorg. Chem.* **2002**, *30*, 303–314. (b) Konar, V.; Yılmaz, Ö.; Aslan, F.; Öztürk, A. İ.; Kırbağ, S.; Arslan, M. *Bioorg. Chem.* **2000**, *28*, 214–225. (c) Öztürk, A. İ.; Yılmaz, Ö.; Kırbağ, S.; Arslan, M. *Cell Biochem. Funct.* **2000**, *18*, 117–126.

(16) (a) Greish, Y. E.; Bender, J. D.; Lakshmi, S.; Brown, P. W.; Allcock, H. R.; Laurencin, C. T. *Biomaterials* **2005**, *26*, 1–9. (b) Nair, L.; Bhattacharyya, S.; Bender, J. D.; Greish, Y. E.; Brown, P. W.; Allcock, H.; Laurencin, C. T. *Biomacromolecules* **2004**, *5*, 2212–2220.

(17) Centreon, C. A. Ph.D. Dissertation, The Ohio State University, Columbus, OH, 2003.

(18) Razafimahefa, D.; Ralambomanana, D. A.; Hammouche, L.; Péliniski, L.; Lauvagie, S.; Bebear, C.; Brocardb, J.; Maugeind, J. *Bioorg. Med. Chem. Lett.* **2005**, *15*, 2301–2303.

(19) (a) Bešli, S.; Coles, S. J.; Davies, D. B.; Eaton, R. J.; Hursthouse, M. B.; Kılıç, A.; Shaw, R. A.; Çiftçi, G. Y.; Yeşilot, S. *J. Am. Chem. Soc.* **2003**, *125*, 4943–4950. (b) Bhuvan Kumar, N. N.; Kumara Swamy, K. C. *Chirality* **2008**, *20*, 781–789.

(20) (a) İlter, E. E.; Çaylak, N.; Işıklan, M.; Asmafiliz, N.; Kılıç, Z.; Hökelek, T. *J. Mol. Struct.* **2004**, *697*, 119–129. (b) Asmafiliz, N.; İlter, E. E.; Işıklan, M.; Kılıç, Z.; Tercan, B.; Çaylak, N.; Hökelek, T.; Büyükgüngör, O. *J. Mol. Struct.* **2007**, *30*, 172–183. (c) Asmafiliz, N.; İlter, E. E.; Kılıç, Z.; Hökelek, T.; Şahin, E. J. *Chem. Sci.* **2008**, *120*(4), 363–376.

(21) (a) Coles, S. J.; Davies, D. B.; Eaton, R. J.; Hursthouse, M. B.; Kılıç, A.; Shaw, R. A.; Şahin, Ş.; Uslu, A.; Yeşilot, S. *Inorg. Chem. Commun.* **2004**, *7*, 657–661. (b) Coles, S. J.; Davies, D. B.; Hursthouse, M. B.; Kılıç, A.; Şahin, Ş.; Shaw, R. A.; Uslu, A. *J. Organomet. Chem.* **2007**, *692*, 2811–2821. (c) İlter, E. E.; Asmafiliz, N.; Kılıç, Z.; Işıklan, M.; Hökelek, T.; Çaylak, N.; Şahin, E. *Inorg. Chem.* **2007**, *46*, 9931–9944.

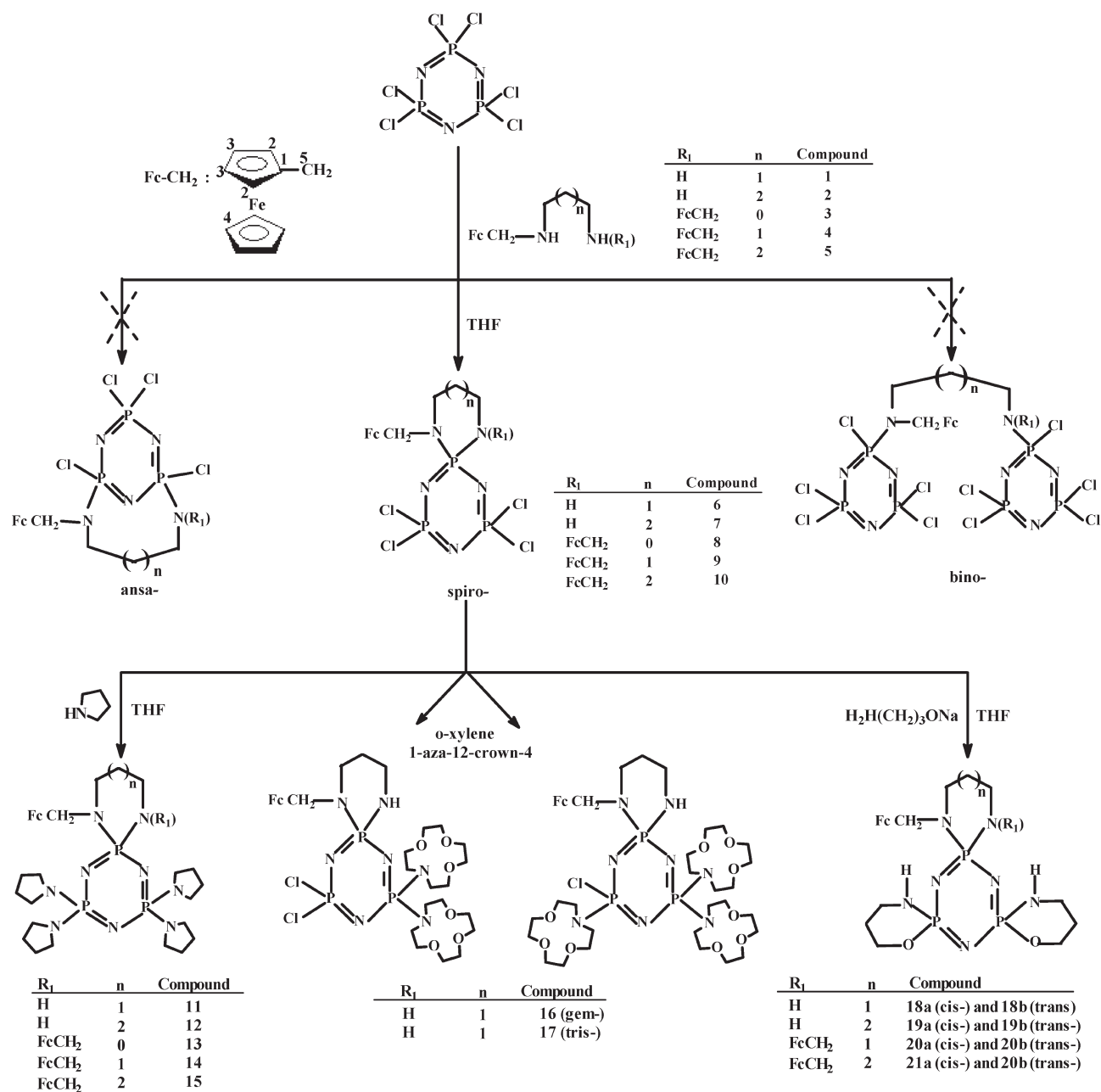
(22) (a) Uslu, A.; Coles, S. J.; Davies, D. B.; Eaton, R. J.; Hursthouse, M. B.; Kılıç, A.; Shaw, R. A. *Eur. J. Inorg. Chem.* **2005**, 1042–1047. (b) Bešli, S.; Coles, S. J.; Davies, D. B.; Eaton, R. J.; Hursthouse, M. B.; Kılıç, A.; Shaw, R. A.; Uslu, A.; Yeşilot, S. *Inorg. Chem. Commun.* **2004**, *7*, 842–846.

(23) Bešli, S.; Davies, D. B.; Kılıç, A.; Shaw, R. A.; Şahin, Ş.; Uslu, A.; Yeşilot, S. *J. Chromatogr., A* **2006**, *1132*, 201–205.

(24) (a) Bui, T. T.; Coles, S. J.; Davies, D. B.; Drake, A. F.; Eaton, R. J.; Hursthouse, M. B.; Kılıç, A.; Shaw, R. A.; Yeşilot, S. *Chirality* **2005**, *17*, 438–443. (b) Yeşilot, S.; Çoşut, B. *Inorg. Chem. Commun.* **2007**, *10*, 88–93.

(25) Prussin, A. J.; Zhao, S.; Jain, A.; Winkel, B. S. J.; Brewer, K. J. *J. Inorg. Biochem.* **2009**, *103*, 427–431.

(26) Turner, P. C.; McLennan, A. G.; Bates, A. D.; White, M. R. H. *Molecular Biology*, 2nd ed.; Springer: Berlin, 2000.

Scheme 1. Chloride Replacement Reaction Pathway of $N_3P_3Cl_6$ with Amines

probe. Standard Bruker pulse programs²⁷ were used in the experiment. IR spectra were recorded on a Mattson 1000 FTIR spectrometer in KBr disks. APIES mass spectrometric analyses were performed on an AGILENT 1100 MSD spectrometer. Mycobacterial susceptibility testing was performed by the BACTEC MGIT 960 (Becton Dickinson, Sparks, MD) system (Supporting Information, section S1). Antituberculosis activity against reference strain *M. tuberculosis* H37Rv (ATCC 27294) was carried out (Supporting Information, section S2). The DNA binding abilities were examined by agarose gel electrophoresis (Supporting Information, section S3).

Preparation of Compounds. Mono- (**1** and **2**) and bisferrocenyldiamines (**3–5**) have been obtained from the reaction of ferrocenecarboxaldehyde with corresponding aliphatic amines according to the methods reported in the literature.²⁸

Spiro(propane-1,3-diamino)[*N*-(1-ferrocenylmethyl)]-4,4,6,6-tetrachlorocyclotriphosphazatriene (6**).** A solution of **1** (1.50 g, 5.52 mmol) in tetrahydrofuran (THF; 150 mL) and triethylamine (1.56 mL) was added to a stirred solution of $N_3P_3Cl_6$ (1.92 g, 5.52 mmol) in THF (50 mL) at room temperature. The mixture was stirred for 25 h, and the precipitated triethylamine hydrochloride was filtered off. The solvent was evaporated, and the product was purified by column chromatography with toluene. Orange powder was crystallized from *n*-heptane (toluene, $R_f = 0.41$). Yield: 2.10 g (70%). Mp: 130 °C. Anal. Calcd for $C_{14}H_{18}N_5FeP_3Cl_4$: C, 30.75; H, 3.32; N, 12.81. Found: C, 31.50; H, 3.75; N, 12.79. APIES-MS (fragments are based on ^{35}Cl and ^{56}Fe , Ir %): m/z 546 ($[MH]^+$, 0.2), 332 ($[M - (FeCH_2NH_2)]^+$, 100.0). FTIR (KBr, cm^{-1}): ν 3308, 3211

(28) (a) Kim, E.; Kwon, S.; Shim, S.; Kim, T.; Jeong, J. H. *Bull. Korean Chem. Soc.* **1997**, *18*, 579–584. (b) Schuhmann, W.; Ohara, T. J.; Schmidt, H.; Heller, A. *J. Am. Chem. Soc.* **1991**, *113*, 1394–1397. (c) Neuse, E. W.; Meirink, M. G.; Blorn, N. F. *Organometallics* **1988**, *7*, 2562–2565.

(27) Bruker program 1D WIN-NMR (release 6.0) and 2D WIN-NMR (release 6.1).

(N–H), 3094, 3074 (C–H aromatic), 2995, 2872 (C–H aliphatic), 1236, 1188 (P=N), 569, 509 (PCL). ¹H NMR (500 MHz, CDCl₃, ppm; numbering of hydrogen atoms is given in Scheme 1): δ 4.28 (dd, 2H, ³J_{HH} = 3.0 Hz, ⁴J_{HH} = 1.5 Hz, H2), 4.14 (bp, 2H, H3), 4.14 (bp, 5H, H4), 3.84 (d, 2H, ³J_{PH} = 9.9 Hz, H5), 3.21 (m, 2H, ³J_{PH} = 16.2 Hz, NCH₂), 3.04 (m, 2H, ³J_{PH} = 14.1 Hz, NHCH₂), 2.61 (bp, 1H, NH), 1.72 (m, 2H, NCH₂CH₂). ¹³C NMR (500 MHz, CDCl₃, ppm; numbering of C atoms is given in Scheme 1): δ 82.44 (d, ³J_{PC} = 9.0 Hz, C1), 69.93 (s, C2), 69.40 (s, C3), 68.65 (s, C4), 47.00 (d, ²J_{PC} = 2.6 Hz, C5), 45.48 (s, NCH₂), 40.71 (d, ²J_{PC} = 3.3 Hz, NHCH₂), 26.44 (d, ³J_{PC} = 5.0 Hz, NCH₂CH₂).

Spiro(butane-1,4-diamino)[N-(1-ferrocenylmethyl)]-4,4,6,6-tetrachlorocyclotriphosphazatriene (7). The workup procedure was similar to that of compound **6**, using **2** (1.65 g, 5.77 mmol), N₃P₃Cl₆ (2.00 g, 5.77 mmol), and triethylamine (1.62 mL) (toluene, R_f = 0.55). Yield: 2.22 g (69%). Mp: 152–154 °C. Anal. Calcd for C₁₅H₂₀N₅FeP₃Cl₄: C, 32.12; H, 3.59; N, 12.49. Found: C, 32.93; H, 3.77; N, 12.87. APIES-MS (fragments are based on ³⁵Cl and ⁵⁶Fe, Ir %): m/z 559 ([M]⁺, 56.6). FTIR (KBr, cm⁻¹): ν 3333, 3240 (N–H), 3096, 3072 (C–H aromatic), 2995, 2878 (C–H aliphatic), 1244, 1186 (P=N), 569, 523 (PCL). ¹H NMR (500 MHz, CDCl₃, ppm; numbering of H atoms is given in Scheme 1): δ 4.28 (dd, 2H, ³J_{HH} = 3.1 Hz, ⁴J_{HH} = 1.6 Hz, H2), 4.14 (bp, 2H, H3), 4.14 (bp, 5H, H4), 4.06 (d, 2H, ³J_{PH} = 12.7 Hz, H5), 3.15 (m, 2H, ³J_{PH} = 16.8 Hz, NCH₂), 3.08 (m, 2H, ³J_{PH} = 12.2 Hz, NHCH₂), 2.80 (bp, 1H, NH), 1.57 (m, 2H, NHCH₂CH₂), 1.49 (m, 2H, NCH₂CH₂). ¹³C NMR (500 MHz, CDCl₃, ppm; numbering of C atoms is given in Scheme 1): δ 84.32 (d, ³J_{PC} = 3.2 Hz, C1), 69.92 (s, C2), 68.56 (s, C4), 68.35 (s, C3), 47.16 (d, ²J_{PC} = 7.4 Hz, C5), 45.36 (d, ²J_{PC} = 7.1, NCH₂), 40.25 (s, NHCH₂), 30.91 (s, NHCH₂CH₂), 27.62 (s, NCH₂CH₂).

Spiro(ethane-1,2-diamino)[N,N'-bis(1-ferrocenylmethyl)]-4,4,6,6-tetrachlorocyclotriphosphazatriene (8). The workup procedure was similar to that of compound **6**, using **3** (2.00 g, 5.81 mmol), N₃P₃Cl₆ (2.02 g, 5.81 mmol), and triethylamine (1.63 mL) (toluene, R_f = 0.52). Yield: 2.80 g (66%). Mp: 211 °C. Anal. Calcd for C₂₄H₂₆N₅FeP₃Cl₄: C, 39.42; H, 3.58; N, 9.58. Found: C, 40.12; H, 3.45; N, 9.38. APIES-MS (fragments are based on ³⁵Cl and ⁵⁶Fe, Ir %): m/z 730 ([MH]⁺, 69.7). FTIR (KBr, cm⁻¹): ν 3092, 3072 (C–H aromatic), 2948, 2859 (C–H aliphatic), 1230, 1184 (P=N), 563, 529 (PCL). ¹H NMR (500 MHz, CDCl₃, ppm; numbering of H atoms is given in Scheme 1): δ 4.26 (4H, H2), 4.14 (bp, 4H, H3), 4.14 (bp, 10H, H4), 3.82 (d, 4H, ³J_{PH} = 10.2 Hz, H5), 3.03 (d, 4H, ³J_{PH} = 10.7 Hz, NCH₂). ¹³C NMR (500 MHz, CDCl₃, ppm; numbering of C atoms is given in Scheme 1): δ 82.40 (d, ³J_{PC} = 8.7 Hz, C1), 69.62 (s, C2), 68.63 (s, C4), 68.45 (s, C3), 43.90 (d, ²J_{PC} = 5.8 Hz, C5), 43.70 (d, ²J_{PC} = 14.8, NCH₂).

Spiro(propane-1,3-diamino)[N,N'-bis(1-ferrocenylmethyl)]-4,4,6,6-tetrachlorocyclotriphosphazatriene (9). The workup procedure was similar to that of compound **6**, using **4** (1.35 g, 2.87 mmol), N₃P₃Cl₆ (1.00 g, 2.87 mmol), and triethylamine (0.81 mL) (toluene, R_f = 0.72). Yield: 1.30 g (61%). Mp: 153 °C. Anal. Calcd for C₂₅H₂₈N₅FeP₃Cl₄: C, 40.31; H, 3.79; N, 9.40. Found: C, 40.72; H, 4.32; N, 9.40. APIES-MS (fragments are based on ³⁵Cl and ⁵⁶Fe, Ir %): m/z 744 ([MH]⁺, 1.6). FTIR (KBr, cm⁻¹): ν 3092, 3072 (C–H aromatic), 2941, 2849 (C–H aliphatic), 1230, 1176 (P=N), 571, 517 (PCL). ¹H NMR (500 MHz, CDCl₃, ppm; numbering of H atoms is given in Scheme 1): δ 4.28 (dd, 4H, ³J_{HH} = 3.6 Hz, ⁴J_{HH} = 1.8 Hz, H2), 4.16 (bp, 4H, H3), 4.14 (bp, 10H, H4), 3.86 (d, 4H, ³J_{PH} = 10.0 Hz, H5), 2.88 (m, 4H, ³J_{PH} = 14.5 Hz, ³J_{HH} = 5.9 Hz, NCH₂), 1.62 (m, 2H, ³J_{HH} = 5.9 Hz, NCH₂CH₂). ¹³C NMR (500 MHz, CDCl₃, ppm; numbering of carbons is given in Scheme 1): δ 82.53 (d, ³J_{PC} = 8.7 Hz, C1), 70.03 (s, C2), 68.70 (s, C4), 68.43 (s, C3), 46.79 (d, ²J_{PC} = 3.9 Hz, C5), 45.15 (s, N-CH₂), 24.96 (d, ³J_{PC} = 2.9 Hz, N-CH₂-CH₂).

Spiro(butane-1,4-diamino)[N,N'-bis(1-ferrocenylmethyl)]-4,4,6,6-tetrachlorocyclotriphosphazatriene (10). The workup procedure was similar to that of compound **6**, using **5** (1.64 g,

5.39 mmol), N₃P₃Cl₆ (1.18 g, 3.39 mmol), and triethylamine (0.95 mL) (toluene, R_f = 0.75). Yield: 1.4 g (53%). Mp: 214–216 °C. Anal. Calcd for C₂₆H₃₀N₅FeP₃Cl₄: C, 41.15; H, 3.98; N, 9.23. Found: C, 41.52; H, 4.35; N, 9.59. APIES-MS (fragments are based on ³⁵Cl and ⁵⁶Fe, Ir %): m/z 757 ([M]⁺, 30.3). FTIR (KBr, cm⁻¹): ν 3243 (N–H), 3090, 3078 (C–H aromatic), 2945, 2849 (C–H aliphatic), 1244, 1182 (P=N), 571, 515 (PCL). ¹H NMR (500 MHz, CDCl₃, ppm; numbering of H atoms is given in Scheme 1): δ 4.25 (dd, 4H, ³J_{HH} = 2.2 Hz, ⁴J_{HH} = 1.6 Hz, H2), 4.13 (bp, 4H, H3), 4.13 (bp, 10H, H4), 4.04 (d, 4H, ³J_{PH} = 12.7 Hz, H5), 3.15 (m, 4H, ³J_{PH} = 15.5 Hz, NCH₂), 1.57 (m, 4H, NCH₂CH₂). ¹³C NMR (500 MHz, CDCl₃, ppm; numbering of C atoms is given in Scheme 1): δ 84.39 (d, ³J_{PC} = 3.5 Hz, C1), 69.64 (s, C2), 68.53 (s, C4), 68.30 (s, C3), 46.42 (d, ²J_{PC} = 7.1 Hz, C5), 44.64 (d, ²J_{PC} = 6.7, NCH₂), 26.44 (s, NCH₂CH₂).

Spiro(propane-1,3-diamino)[N-(1-ferrocenylmethyl)]-4,4,6,6-tetrapyrrolidinocyclotriphosphazatriene (11). A solution of compound **6** (1.25 g, 2.29 mmol) in dry THF (150 mL) was added slowly to a solution of pyrrolidine (2.25 mL, 27.0 mmol) with stirring and refluxing for 30 h. After excess triethylamine (1.28 mL, 9.14 mmol) was added to the solution, the mixture was refluxed for 4 h. After the solvent was evaporated, the oily product was purified by column chromatography by using benzene–THF (3:2) as the eluent and was crystallized from *n*-heptane (THF, R_f = 0.55). Yield: 1.00 g (64%). Mp: 158–160 °C. Anal. Calcd for C₃₀H₅₀N₉FeP₃: C, 52.56; H, 7.35; N, 18.39. Found: C, 52.27; H, 7.69; N, 18.33. APIES-MS (fragments are based on ⁵⁶Fe, Ir %): m/z 686 ([M]⁺, 100.0). FTIR (KBr, cm⁻¹): ν 3296, 3231 (N–H), 3092, 3073 (C–H aromatic), 2949, 2859 (C–H aliphatic), 1190 (P=N). ¹H NMR (500 MHz, CDCl₃, ppm; numbering of H atoms is given in Scheme 1): δ 4.18 (m, 2H, H2), 4.02 (m, 2H, H3), 4.00 (m, 5H, H4), 3.69 (d, 2H, ³J_{PH} = 6.0 Hz, H5), 3.10 (m, 2H, NHCH₂), 3.25 and 3.10 [m, 16H, NCH₂(pyrr)], 2.90 (m, 2H, NCH₂), 2.11 (bp, 1H, NH), 1.83 and 1.78 [m, 16H, NCH₂CH₂(pyrr)], 1.57 (m, 2H, NCH₂CH₂). ¹³C NMR (500 MHz, CDCl₃, ppm; numbering of C atoms is given in Scheme 1): δ 84.40 (d, ³J_{PC} = 14.0 Hz, C1), 70.23 (s, C2), 68.27 (s, C4), 67.79 (s, C3), 47.57 (s, C5), 46.30 and 46.00 [s, NCH₂(pyrr)], 46.04 (s, NCH₂), 41.76 (s, NHCH₂), 28.48 (s, NCH₂CH₂), 26.46 [dd, ³J_{PC} = 9.1 Hz, NCH₂CH₂(pyrr)], 26.42 [dd, ³J_{PC} = 9.3 Hz, NCH₂CH₂(pyrr)].

Spiro(butane-1,4-diamino)[N-(1-ferrocenylmethyl)]-4,4,6,6-tetrapyrrolidinocyclotriphosphazatriene (12). The workup procedure was similar to that of compound **11**, using **7** (1.00 g, 1.78 mmol) and pyrrolidine (1.76 mL, 20.00 mmol). After excess triethylamine (1.00 mL, 7.12 mmol) was added to the solution, the mixture was refluxed for 4 h. The product was purified by column chromatography by using benzene–THF (3:1) and was crystallized from *n*-heptane (THF, R_f = 0.65). Yield: 0.75 g (60%). Mp: 96–97 °C. Anal. Calcd for C₃₁H₅₂N₉FeP₃: C, 53.22; H, 7.49; N, 18.02. Found: C, 53.08; H, 7.44; N, 17.87. APIES-MS (fragments are based on ⁵⁶Fe, Ir %): m/z 700 ([M]⁺, 2.1). FTIR (KBr, cm⁻¹): ν 3429, 3273 (N–H), 3094, 3074 (C–H aromatic), 2956, 2861 (C–H aliphatic), 1186 (P=N). ¹H NMR (500 MHz, CDCl₃, ppm; numbering of H atoms is given in Scheme 1): δ 4.25 (dd, 2H, ³J_{HH} = 3.2 Hz, ⁴J_{HH} = 1.6 Hz, H2), 4.10 (m, 2H, H3), 4.08 (m, 5H, H4), 4.06 (dd, 2H, ³J_{PH} = 3.5 Hz, H5), 2.97 (m, 2H, NCH₂), 2.95 (m, 2H, NHCH₂), 3.22 and 3.14 [m, 16H, NCH₂(pyrr)], 2.10 (bp, 1H, NH), 1.83 and 1.78 [m, 16H, NCH₂CH₂(pyrr)], 1.47 (m, 2H, NHCH₂CH₂), 1.40 (m, 2H, NCH₂CH₂). ¹³C NMR (500 MHz, CDCl₃, ppm; numbering of C atoms is given in Scheme 1): δ 86.75 (s, C1), 69.64 (s, C2), 68.23 (s, C4), 67.58 (s, C3), 46.96 (d, ²J_{PC} = 5.2 Hz, C5), 46.32 and 46.10 [s, NCH₂(pyrr)], 44.80 (s, NCH₂), 40.28 (s, NHCH₂), 31.90 (s, NHCH₂CH₂), 28.01 (s, NCH₂CH₂), 26.42 [d, ³J_{PC} = 9.4 Hz, NCH₂CH₂(pyrr)], 26.38 [d, ³J_{PC} = 9.5 Hz, NCH₂CH₂(pyrr)].

Spiro(ethane-1,2-diamino)[N,N'-bis(1-ferrocenylmethyl)]-4,4,6,6-tetrapyrrolidinocyclotriphosphazatriene (13). The workup procedure was similar to that of compound **11**, using **8** (1.10 g,

1.50 mmol) and pyrrolidine (1.48 mL, 18.00 mmol). After excess triethylamine (0.85 mL, 6.02 mmol) was added to the solution, the mixture was refluxed for 4 h. The product was purified by column chromatography by using benzene–THF (3:1) and was crystallized from *n*-heptane (THF, $R_f = 0.75$). Yield: 0.55 g (42%). Mp: 232 °C. Anal. Calcd for $C_{40}H_{58}N_9Fe_2P_3 \cdot H_2O$: C, 54.13; H, 6.81; N, 14.20. Found: C, 54.50; H, 6.21; N, 13.82. APIES-MS (fragments are based on ^{56}Fe , Ir %): m/z 870 ($[M]^+$, 0.4). FTIR (KBr, cm^{-1}): ν 3092, 3073 (C–H aromatic), 2949, 2837 (C–H aliphatic), 1188 (P=N). 1H NMR (500 MHz, $CDCl_3$, ppm; numbering of H atoms is given in Scheme 1): δ 4.28 (dd 4H, $^3J_{HH} = 3.3$ Hz, $^4J_{HH} = 1.6$ Hz, H2), 4.11 (m, 4H, H3), 4.07 (m, 10H, H4), 3.78 (d, 4H, $^3J_{PH} = 5.1$ Hz, H5), 3.28 [m, 16H, NCH_2 (pyrr)], 2.86 (d, 4H, $^3J_{PH} = 10.6$ Hz, NCH_2), 1.90 [m, 16H, NCH_2CH_2 (pyrr)]. ^{13}C NMR (500 MHz, $CDCl_3$, ppm; numbering of C atoms is given in Scheme 1): δ 84.94 (s, C1), 69.62 (s, C2), 68.63 (s, C4), 68.46 (s, C3), 45.33 (d, $^2J_{PC} = 5.1$ Hz, C5), 46.34 [s, NCH_2 (pyrr)], 46.34 (s, NCH_2), 26.50 [dd, $^3J_{PC} = 9.5$ Hz, NCH_2CH_2 (pyrr)].

Spiro(propane-1,3-diamino)[*N,N'*-bis(1-ferrocenylmethyl)]-4,4,6,6-tetrapyrrolidinocyclotriphosphazatriene (14). The workup procedure was similar to that of compound **11**, using **9** (1.00 g, 1.34 mmol) and pyrrolidine (1.15 mL, 16.00 mmol). After excess triethylamine (0.75 mL, 5.36 mmol) was added to the solution, the mixture was refluxed for 4 h. After the solvent was evaporated, the crude product was purified by column chromatography with benzene–THF (3:1) and was crystallized from *n*-heptane (THF, $R_f = 0.80$). Yield: 0.75 g (63%). Mp: 156–157 °C. Anal. Calcd for $C_{41}H_{60}N_9Fe_2P_3$: C, 55.73; H, 6.84; N, 14.27. Found: C, 55.28; H, 7.01; N, 14.07. APIES-MS (fragments are based on ^{56}Fe , Ir %): m/z 884 ($[M]^+$, 100.0). FTIR (KBr, cm^{-1}): ν 3090, 3079 (C–H aromatic), 2947, 2839 (C–H aliphatic), 1188 (P=N). 1H NMR (500 MHz, $CDCl_3$, ppm; numbering of H atoms is given in Scheme 1): δ 4.19 (dd 4H, $^3J_{HH} = 3.5$ Hz, $^4J_{HH} = 1.8$ Hz, H2), 4.08 (m, 4H, H3), 4.08 (m, 10H, H4), 3.85 (d, 4H, $^3J_{PH} = 5.6$ Hz, H5), 3.28 [m, 16H, NCH_2 (pyrr)], 2.92 (m, 4H, $^3J_{PH} = 14.6$ Hz, NCH_2), 1.88 [m, 16H, NCH_2CH_2 (pyrr)], 1.50 (m, 2H, CH_2CH_2). ^{13}C NMR (500 MHz, $CDCl_3$, ppm; numbering of C atoms is given in Scheme 1): δ 84.96 (d, $^3J_{PC} = 14.3$ Hz, C1), 70.27 (s, C2), 68.30 (s, C4), 67.74 (s, C3), 46.38 (d, $^2J_{PC} = 5.7$ Hz, C5), 46.47 [d, $^2J_{PC} = 4.4$ Hz, NCH_2 (pyrr)], 45.28 (s, NCH_2), 26.53 [dd, $^3J_{PC} = 9.5$ Hz, NCH_2CH_2 (pyrr)], 23.26 (d, $^3J_{PC} = 2.7$ Hz, NCH_2CH_2).

Spiro(butane-1,4-diamino)[*N,N'*-bis(1-ferrocenylmethyl)]-4,4,6,6-tetrapyrrolidinocyclotriphosphazatriene (15). The workup procedure was similar to that of compound **11**, using **10** (0.66 g, 0.87 mmol) and pyrrolidine (0.74 mL, 10.00 mmol). After excess triethylamine (0.49 mL, 3.49 mmol) was added to the solution, the mixture was refluxed for 4 h (THF, $R_f = 0.83$). Yield: 0.45 g (58%). Mp: 167 °C. Anal. Calcd for $C_{42}H_{62}N_9Fe_2P_3$: C, 56.20; H, 6.96; N, 14.04. Found: C, 56.09; H, 6.69; N, 13.81. APIES-MS (fragments are based on ^{56}Fe , Ir %): m/z 898 ($[M]^+$, 100.0). FTIR (KBr, cm^{-1}): ν 3252 (N–H), 3090, 3078 (C–H aromatic), 2949, 2841 (C–H aliphatic), 1186 (P=N). 1H NMR (500 MHz, $CDCl_3$, ppm; numbering of H atoms is given in Scheme 1): δ 4.19 (dd 4H, $^3J_{HH} = 3.4$ Hz, $^4J_{HH} = 1.7$ Hz, H2), 4.08 (d, 4H, $^3J_{PH} = 7.4$ Hz, H5), 4.07 (m, 10H, H4), 4.06 (m, 4H, H3), 3.20 [m, 16H, NCH_2 (pyrr)], 2.98 (m, 4H, $^3J_{PH} = 15.0$ Hz, NCH_2), 1.83 [m, 16H, NCH_2CH_2 (pyrr)], 1.13 (m, 4H, NCH_2CH_2). ^{13}C NMR (500 MHz, $CDCl_3$, ppm; numbering of C atoms is given in Scheme 1): δ 86.74 (d, $^3J_{PC} = 6.8$ Hz, C1), 69.80 (s, C2), 68.18 (s, C4), 67.61 (s, C3), 46.30 (s, C5), 46.30 [s, NCH_2 (pyrr)], 44.05 (d, $^2J_{PC} = 5.9$ Hz, NCH_2), 26.40 [dd, $^3J_{PC} = 9.5$ Hz, NCH_2CH_2 (pyrr)], 26.18 (s, NCH_2CH_2).

Spiro(propane-1,3-diamino)[*N*-(1-ferrocenylmethyl)]-4,4-bis-(1-aza-4,7,10-trioxadodecanyl)-6,6-dichlorocyclotriphosphazatriene (16). To an *o*-xylene (100 mL) solution of **6** (0.90 g, 1.66 mmol) was added triethylamine (0.47 mL) and 1-aza-12-crown-4 (0.58 g, 3.33 mmol), and the mixture was refluxed for 4 h. After

o-xylene was evaporated, the oily residue was chromatographed [silica gel, eluent toluene–THF (7:1); THF, $R_f = 0.71$]. Yield: 0.72 g (53%). Anal. Calcd for $C_{30}H_{50}N_7O_6FeP_3Cl_2$: C, 43.71; H, 6.11; N, 11.89. Found: C, 43.79; H, 5.86; N, 11.75. APIES-MS (fragments are based on ^{35}Cl and ^{56}Fe , Ir %): m/z 824 ($[MH]^+$, 100.0). FTIR (KBr, cm^{-1}): ν 3313 (N–H), 3095 (C–H aromatic), 2930, 2860 (C–H aliphatic), 1221 (P=N), 532, 508 (PCl). 1H NMR (500 MHz, $CDCl_3$, ppm; numbering of H atoms is given in Scheme 1): δ 4.28 and 4.24 (m, 2H, H2), 4.15 (m, 5H, H4), 4.12 (m, 2H, H3), 3.98–3.31 (m, 24H, OCH_2), 3.98–3.31 (m, 2H, H5), 3.98–3.31 (m, 2H, NCH_2), 3.98–3.31 (m, 2H, $NHCH_2$), 3.98–3.31 [m, 8H, NCH_2 (crown ether)], 2.20 (bp, 1H, NH), 1.84 (m, 2H, NCH_2CH_2). ^{13}C NMR (500 MHz, $CDCl_3$, ppm; numbering of C atoms is given in Scheme 1): δ 83.40 (d, $^3J_{PC} = 11.9$ Hz, C1), 70.11 and 69.63 (s, C2), 68.15 and 67.92 (s, C3), 71.49, 70.99, 70.88, 70.55, and 69.86 (s, OCH_2), 71.30 (d, $^3J_{PC} = 3.7$ Hz, OCH_2), 68.49 (s, C4), 49.33 [d, $^2J_{PC} = 4.3$ Hz, NCH_2 (crown ether)], 47.34 [d, $^2J_{PC} = 3.6$ Hz, NCH_2 (crown ether)], 46.66 (s, C5), 45.92 (s, NCH_2), 41.10 (d, $^2J_{PC} = 4.2$ Hz, $NHCH_2$), 26.79 (d, $^3J_{PC} = 3.8$ Hz, NCH_2CH_2).

Spiro(propane-1,3-diamino)[*N*-(1-ferrocenylmethyl)]-4,4,6-tris(1-aza-4,7,10-trioxadodecanyl)-6-chlorocyclotriphosphazatriene (17). To an *o*-xylene (100 mL) solution of **6** (0.67 g, 1.23 mmol) was added triethylamine (0.69 mL) and 1-aza-12-crown-4 (0.65 g, 3.69 mmol), and the mixture was refluxed for 7 h. After complete evaporation of the solvent, the oily residue was purified by column chromatography with toluene–THF (7:1) (THF, $R_f = 0.82$). Yield: 0.40 g (34%). Anal. Calcd for $C_{38}H_{66}N_8O_9FeP_3Cl \cdot H_2O$: C, 46.53; H, 6.93; N, 11.42. Found: C, 46.34; H, 7.21; N, 11.10. APIES-MS (fragments are based on ^{35}Cl and ^{56}Fe , Ir %): m/z 824 ($[M - (C_5H_{11}O_2 + Cl)]^+$, 100.0). FTIR (KBr, cm^{-1}): ν 3425 (N–H), 3090, 3078 (C–H aromatic), 2914, 2861 (C–H aliphatic), 1230 (P=N), 563 (PCl). 1H NMR (500 MHz, $CDCl_3$, ppm; numbering of H atoms is given in Scheme 1): δ 4.26 and 4.22 (m, 2H, H2), 4.15 and 4.12 (m, 2H, H3), 4.15 (m, 5H, H4), 4.10–3.50 (m, 36H, OCH_2), 3.83 (m, 2H, H5), 3.50–2.80 (m, 2H, NCH_2), 3.50–2.80 (m, 2H, $NHCH_2$), 3.50–2.80 [m, 12H, NCH_2 (crown ether)], 2.30 (bp, 1H, NH), 1.46 (m, 2H, NCH_2CH_2). ^{13}C NMR (500 MHz, $CDCl_3$, ppm; numbering of C atoms is given in Scheme 1): δ 83.18 (d, $^3J_{PC} = 13.2$ Hz, C1), 70.78 and 69.93 (s, C2), 68.52 (s, C4), 68.25 and 67.97 (s, C3), 71.44, 71.2, 70.90, 70.61, 70.13, and 69.57 (s, OCH_2), 49.48 [d, $^2J_{PC} = 2.7$ Hz, NCH_2 (crown ether)], 47.34 [d, $^2J_{PC} = 2.7$ Hz, NCH_2 (crown ether)], 46.61 (s, C5), 45.97 (s, NCH_2), 41.16 (d, $^2J_{PC} = 4.0$ Hz, $NHCH_2$), 30.33 (s, NCH_2CH_2).

Spiro(propane-1,3-diamino)[*N*-(1-ferrocenylmethyl)]-*cis*-bis-[spiro(propane-3-amino-1-oxy)cyclotriphosphazatriene (18a) and Spiro(propane-1,3-diamino)[*N*-(1-ferrocenylmethyl)]-*trans*-bis-[spiro(propane-3-amino-1-oxy)cyclotriphosphazatriene (18b)]. To a THF (150 mL) solution of **6** (1.43 g, 2.61 mmol) was added sodium (3-amino-1-propanoxide) (0.39 g, 5.23 mmol) and triethylamine (1.47 mL) at room temperature. The mixture was refluxed for 24 h, and the precipitated triethylamine hydrochloride and sodium chloride were filtered off. The solvent was evaporated completely, and the oily residue was purified by column chromatography using dichloromethane–THF (7:3) as the eluent. Two isomeric compounds were isolated. The first one was the *cis* isomer (**18a**; THF, $R_f = 0.69$). Yield: 0.30 g (21%). Mp: 261 °C. Anal. Calcd for $C_{20}H_{32}N_7O_2FeP_3$: C, 43.58; H, 5.84; N, 17.79. Found: C, 43.21; H, 5.63; N, 18.03. APIES-MS (fragments are based on ^{56}Fe , Ir %): m/z 552 ($[MH]^+$, 100.0). FTIR (KBr, cm^{-1}): ν 3318 (N–H), 3091, 3072 (C–H aromatic), 2946, 2841 (C–H aliphatic), 1198 (P=N). 1H NMR (500 MHz, $CDCl_3$, ppm; numbering of H atoms is given in Scheme 1): δ 4.40 (m, 4H, OCH_2), 4.27 (dd, 2H, $^3J_{HH} = 3.3$ Hz, $^4J_{HH} = 1.6$ Hz, H2), 4.12 (m, 5H, H4), 4.09 (m, 2H, H3), 3.81 (d, 2H, $^3J_{PH} = 9.6$ Hz, H5), 3.42 (m, 4H, $NHCH_2$), 3.22 (m, 2H, NCH_2), 3.04 [m, 2H, $^3J_{PH} = 13.3$ Hz, $NHCH_2$ (NN-spiro)], 2.47 (bp, 2H, NH),

2.42 (bp, 1H, *NH*), 1.81 (m, 4H, OCH_2CH_2), 1.67 (m, 2H, NCH_2CH_2). ^{13}C NMR (500 MHz, CDCl_3 , ppm; numbering of C atoms is given in Scheme 1): δ 84.45 (d, $^3J_{\text{PC}} = 7.5$ Hz, C1), 69.79 (s, C2), 68.55 (s, C4), 67.74 (s, C3), 66.95 (bp, OCH_2), 47.46 (s, C5), 46.85 (s, NCH_2), 41.44 [s, NHCH_2 (NN-spiro)], 41.44 (s, NHCH_2), 27.33 (s, NCH_2CH_2), 26.40 [s, OCH_2CH_2].

The second one was the trans compound (**18b**; THF, $R_f = 0.29$). Yield: 0.81 g (56%). Mp: 220 °C. Anal. Calcd for $\text{C}_{20}\text{H}_{32}\text{N}_7\text{O}_2\text{FeP}_3$: C, 43.58; H, 5.84; N, 17.79. Found: C, 43.55; H, 5.82; N, 17.39. APIES-MS (fragments are based on ^{56}Fe , Ir %): m/z 552 ($[\text{MH}]^+$, 100.0). FTIR (KBr, cm^{-1}): ν 3235, 3281 (N–H), 3084, 3075 (C–H aromatic), 2947, 2862 (C–H aliphatic), 1203 (P=N). ^1H NMR (500 MHz, CDCl_3 , ppm; numbering of H atoms is given in Scheme 1): δ 4.48 and 4.39 (m, 4H, OCH_2), 4.28 (dd, 2H, $^3J_{\text{HH}} = 3.5$ Hz, $^4J_{\text{HH}} = 1.8$ Hz, H2), 4.12 (m, 5H, H4), 4.09 and 4.07 (m, 2H, H3), 3.81 (m, 2H, $^3J_{\text{PH}} = 11.2$ Hz, $^2J_{\text{HH}} = 14.0$ Hz, H5), 3.43 and 3.36 (m, 4H, NHCH_2), 3.23 and 3.17 (m, 2H, NCH_2), 3.03 and 2.97 [m, 2H, NHCH_2 (NN-spiro)], 2.55 (bp, 1H, *NH*), 2.44 (bp, 2H, *NH*), 1.87 (m, 2H, NCH_2CH_2), 1.67 (m, 4H, $\text{OCH}_2\text{-CH}_2$). ^{13}C NMR (500 MHz, CDCl_3 , ppm; numbering of C atoms is given in Scheme 1): δ 84.50 (d, $^3J_{\text{PC}} = 8.8$ Hz, C1), 70.04 and 69.77 (s, C2), 68.55 (s, C4), 68.05 and 67.47 (s, C3), 66.95 (bp, OCH_2), 47.23 (s, C5), 46.55 (s, NCH_2), 41.58 [d, $^2J_{\text{PC}} = 4.2$ Hz, NHCH_2 (NN-spiro)], 41.32 (s, NHCH_2), 27.46 (d, $^3J_{\text{PC}} = 4.2$ Hz, $\text{NCH}_2\text{-CH}_2$), 26.24 [d, $^3J_{\text{PC}} = 2.5$ Hz, OCH_2CH_2].

Spiro(butane-1,4-diamino)[N-(1-ferrocenylmethyl)]-cis-bis[spiro(propane-3-amino-1-oxy)]cyclotriphosphazatriene (19a) and Spiro(butane-1,4-diamino)[N-(1-ferrocenylmethyl)]-trans-bis[spiro(propane-3-amino-1-oxy)]cyclotriphosphazatriene (19b). The workup procedure was similar to that of compound **18**, using **7** (1.50 g, 2.67 mmol), sodium (3-amino-1-propanoxide) (0.40 g, 5.35 mmol), and triethylamine (1.51 mL). The solvent was evaporated completely, and the oily residue was chromatographed [silica gel, eluent dichloromethane–THF (7:1)]. Two isomeric compounds were isolated. The first one was the cis isomer (**19a**; THF, $R_f = 0.65$). Yield: 0.60 g (40%). Mp: 231 °C. Anal. Calcd for $\text{C}_{21}\text{H}_{34}\text{N}_7\text{O}_2\text{FeP}_3$: C, 44.62; H, 6.06; N, 17.34. Found: C, 44.82; H, 6.26; N, 17.39. APIES-MS (fragments are based on ^{56}Fe , Ir %): m/z 566 ($[\text{MH}]^+$, 9.1). FTIR (KBr, cm^{-1}): ν 3366, 3203 (N–H), 3087, 3077 (C–H aromatic), 2930, 2850 (C–H aliphatic), 1219 (P=N). ^1H NMR (500 MHz, CDCl_3 , ppm; numbering of H atoms is given in Scheme 1): δ 4.42 (m, 4H, OCH_2), 4.38 and 4.28 (bp, 2H, H2), 4.06 (m, 2H, H3), 4.15 (m, 5H, H4), 4.18 (dd, 1H, $^3J_{\text{PH}} = 10.0$ Hz, $^2J_{\text{HH}} = 14.8$ Hz, H5), 3.96 (dd, 1H, $^3J_{\text{PH}} = 10.1$ Hz, $^2J_{\text{HH}} = 14.8$ Hz, H5), 3.39 (m, 4H, NHCH_2), 3.27–2.94 (m, 2H, NCH_2), 3.27–2.94 [m, 2H, NHCH_2 (NN-spiro)], 2.51 (bp, 3H, *NH*), 1.85 (m, 2H, NCH_2CH_2), 1.72 (m, 4H, OCH_2CH_2), 1.50 [m, 2H, NHCH_2CH_2 (NN-spiro)]. ^{13}C NMR (500 MHz, CDCl_3 , ppm; numbering of C atoms is given in Scheme 1): δ 86.60 (d, $^3J_{\text{PC}} = 2.7$ Hz, C1), 69.74 and 69.63 (s, C2), 68.38 (s, C4), 67.87 and 67.66 (s, C3), 66.76 (d, $^2J_{\text{PC}} = 5.5$ Hz, OCH_2), 66.57 (d, $^2J_{\text{PC}} = 5.4$ Hz, OCH_2), 46.92 (d, $^2J_{\text{PC}} = 6.3$ Hz, C5), 45.04 (s, NCH_2), 41.33 (d, $^2J_{\text{PC}} = 2.6$ Hz, NHCH_2), 41.23 (d, $^2J_{\text{PC}} = 2.8$ Hz, NHCH_2), 40.20 [s, NHCH_2 (NN-spiro)], 31.74 [s, NHCH_2CH_2 (NN-spiro)], 27.90 (s, NCH_2CH_2), 26.36 (dd, $^3J_{\text{PC}} = 7.4$ Hz, OCH_2CH_2).

The second one was the trans compound (**19b**; THF, $R_f = 0.28$). Yield: 0.72 g (48%). Mp: 136 °C. Anal. Calcd for $\text{C}_{21}\text{H}_{34}\text{N}_7\text{O}_2\text{FeP}_3 \cdot \text{H}_2\text{O}$: C, 43.22; H, 6.17; N, 16.80. Found: C, 43.53; H, 6.37; N, 16.42. APIES-MS (fragments are based on ^{56}Fe , Ir %): m/z 566 ($[\text{MH}]^+$, 100.0). FTIR (KBr, cm^{-1}): ν 3322, 3182 (N–H), 3090 (C–H aromatic), 2946, 2850 (C–H aliphatic), 1210, 1198 (P=N). ^1H NMR (500 MHz, CDCl_3 , ppm; numbering of H atoms is given in Scheme 1): δ 4.46 (m, 4H, OCH_2), 4.40 (m, 1H, $^3J_{\text{HH}} = 2.1$ Hz, $^4J_{\text{HH}} = 1.1$ Hz, H2), 4.29 (m, 1H, $^3J_{\text{HH}} = 2.1$ Hz, $^4J_{\text{HH}} = 1.1$ Hz, H2), 4.20 (dd, 1H, $^3J_{\text{PH}} = 9.9$ Hz, $^2J_{\text{HH}} = 14.9$ Hz, H5), 4.12 (m, 5H, H4), 4.08 (m, 2H, H3), 3.97 (dd, 1H, $^3J_{\text{PH}} = 9.9$ Hz, $^2J_{\text{HH}} = 14.9$ Hz, H5), 3.41

(m, 4H, NHCH_2), 3.24 (m, 2H, NCH_2), 3.03 [m, 2H, NHCH_2 (NN-spiro)], 2.48 (bp, 2H, *NH*), 2.32 (bp, 1H, *NH*), 1.86 (m, 2H, NCH_2CH_2), 1.74 (m, 2H, OCH_2CH_2), 1.55 (m, 2H, OCH_2CH_2), 1.45 [m, 2H, $\text{NHCH}_2\text{-CH}_2$ (NN-spiro)]. ^{13}C NMR (500 MHz, CDCl_3 , ppm; numbering of C atoms is given in Scheme 1): δ 86.45 and 85.57 (d, $^3J_{\text{PC}} = 2.3$ Hz, C1), 69.96, 69.82, 69.70, and 69.62 (s, C2), 68.46 and 68.40 (s, C4), 68.02 and 67.92 (s, C3), 66.94 (d, $^2J_{\text{PC}} = 5.2$ Hz, OCH_2), 66.76 (d, $^2J_{\text{PC}} = 5.1$ Hz, OCH_2), 47.02 (d, $^2J_{\text{PC}} = 6.6$ Hz, C5), 46.90 (d, $^2J_{\text{PC}} = 6.2$ Hz, C5), 45.10 (d, $^2J_{\text{PC}} = 5.9$ Hz, NCH_2), 44.85 (d, $^2J_{\text{PC}} = 5.9$ Hz, NCH_2), 41.32 (s, NHCH_2), 41.21 (s, NHCH_2), 40.22 and 40.10 [s, NHCH_2 (NN-spiro)], 36.56 and 34.23 [s, OCH_2CH_2], 32.38 and 31.60 [s, NHCH_2CH_2 (NN-spiro)], 27.88 and 27.48 [s, NCH_2CH_2].

Spiro(propane-1,3-diamino)[N,N'-bis(1-ferrocenylmethyl)]-cis-bis[spiro(propane-3-amino-1-oxy)]cyclotriphosphazatriene (20a) and Spiro(propane-1,3-diamino)[N,N'-bis(1-ferrocenylmethyl)]-trans-bis[spiro(propane-3-amino-1-oxy)]cyclotriphosphazatriene (20b). The workup procedure was similar to that of compound **18**, using **9** (1.14 g, 1.53 mmol), sodium (3-amino-1-propanoxide) (0.23 g, 3.06 mmol), and triethylamine (0.86 mL). The solvent was evaporated completely, and the oily residue was chromatographed [silica gel, eluent dichloromethane–THF (7:1)]. Two isomeric compounds were isolated. The first one was the cis isomer (**20a**; THF, $R_f = 0.65$). Yield: 0.55 g (48%). Mp: 208–210 °C. Anal. Calcd for $\text{C}_{31}\text{H}_{42}\text{N}_7\text{O}_2\text{Fe}_2\text{P}_3$: C, 49.69; H, 5.65; N, 13.08. Found: C, 49.98; H, 6.10; N, 12.87. APIES-MS (fragments are based on ^{56}Fe , Ir %): m/z 566 ($[\text{MH} - \text{Fc}]^+$, 100.0); 676 ($[\text{M} - (\text{C}_3\text{H}_7\text{NO})]^+$, 2.0). FTIR (KBr, cm^{-1}): ν 3354, 3229 (N–H), 3086, 3073 (C–H aromatic), 2951, 2855 (C–H aliphatic), 1219 (P=N). ^1H NMR (500 MHz, CDCl_3 , ppm; numbering of H atoms is given in Scheme 1): δ 4.46 (m, 4H, OCH_2), 4.33 (m, 2H, $^3J_{\text{HH}} = 2.3$ Hz, $^4J_{\text{HH}} = 1.2$ Hz, H2), 4.27 (m, 2H, $^3J_{\text{HH}} = 2.3$ Hz, $^4J_{\text{HH}} = 1.2$ Hz, H2), 4.11 (m, 10H, H4), 4.07 and 4.06 (m, 4H, H3), 3.99 (dd, 2H, $^3J_{\text{PH}} = 8.0$ Hz, $^2J_{\text{HH}} = 14.2$ Hz, H5), 3.69 (dd, 2H, $^3J_{\text{PH}} = 11.9$ Hz, $^2J_{\text{HH}} = 14.2$ Hz, H5), 3.40 (m, 4H, NHCH_2), 3.02 and 2.89 (m, 4H, NCH_2), 2.40 (bp, 2H, *NH*), 1.85 (m, 4H, OCH_2CH_2), 1.65 (m, 2H, NCH_2CH_2). ^{13}C NMR (500 MHz, CDCl_3 , ppm; numbering of C atoms is given in Scheme 1): δ 84.72 (d, $^3J_{\text{PC}} = 9.7$ Hz, C1), 70.06 and 70.01 (s, C2), 68.54 (s, C4), 67.87 and 67.51 (s, C3), 66.84 (s, OCH_2), 47.04 (d, $^2J_{\text{PC}} = 2.1$ Hz, C5), 46.27 (s, NCH_2), 41.34 (s, NHCH_2), 26.45 (dd, $^3J_{\text{PC}} = 5.8$ Hz, OCH_2CH_2), 25.55 (s, NCH_2CH_2).

The second one was the trans compound (**20b**; THF, $R_f = 0.53$). Yield: 0.37 g (42%). Mp: 180–181 °C. Anal. Calcd for $\text{C}_{31}\text{H}_{42}\text{N}_7\text{O}_2\text{Fe}_2\text{P}_3 \cdot \text{C}_7\text{H}_8$: C, 54.24; H, 5.99; N, 11.65. Found: C, 54.11; H, 6.22; N, 11.17. APIES-MS (fragments are based on ^{56}Fe , Ir %): m/z 750 ($[\text{M} + \text{H}]^+$, 100.0). FTIR (KBr, cm^{-1}): ν 3324, 3243 (N–H), 3093 (C–H aromatic), 2918, 2850 (C–H aliphatic), 1200 (P=N). ^1H NMR (500 MHz, CDCl_3 , ppm; numbering of H atoms is given in Scheme 1): δ 4.39 (m, 4H, OCH_2), 4.19 (m, 4H, $^3J_{\text{HH}} = 3.9$ Hz, $^4J_{\text{HH}} = 1.9$ Hz, H2), 4.09 and 3.97 (m, 4H, H3), 4.05 (m, 10H, H4), 3.81 (d, 2H, H5, $^3J_{\text{PH}} = 7.4$ Hz), 3.69 (d, 2H, H5, $^3J_{\text{PH}} = 10.9$ Hz), 3.35 (m, 4H, NHCH_2), 2.92–2.80 (m, 4H, NCH_2), 2.40 (bp, 2H, *NH*), 1.76 (m, 2H, NCH_2CH_2), 1.35 (m, 4H, OCH_2CH_2). ^{13}C NMR (500 MHz, CDCl_3 , ppm; numbering of C atoms is given in Scheme 1): δ 84.95 (s, C1), 70.12 and 69.84 (s, C2), 68.56 and 68.52 (s, C4), 67.69 and 67.65 (s, C3), 66.72 and 66.68 (s, OCH_2), 47.50 and 46.50 (C5), 46.21 and 45.41 (s, NCH_2), 41.41 (s, NHCH_2), 29.90 and 30.11 (s, OCH_2CH_2), 25.55 (s, NCH_2CH_2).

Spiro(butane-1,4-diamino)[N,N'-bis(1-ferrocenylmethyl)]-cis-bis[spiro(propane-3-amino-1-oxy)]cyclotriphosphazatriene (21a) and Spiro(butane-1,3-diamino)[N,N'-bis(1-ferrocenylmethyl)]-trans-bis[spiro(propane-3-amino-1-oxy)]cyclotriphosphazatriene (21b). The workup procedure was similar to that of compound **18**, using **10** (0.58 g, 0.76 mmol), sodium (3-amino-1-propanoxide) (0.11 g, 1.53 mmol), and triethylamine (0.43 mL).

Table 1. Selected Bond Lengths (Å) and Angles (deg) for **7**, **10**, **11**, and **15**

| | 7 | 10 | 11 | 11' | 15 |
|----------|------------|------------|------------|------------|------------|
| P1–N1 | 1.582(3) | 1.580(3) | 1.592(3) | 1.594(3) | 1.597(4) |
| P1–N3 | 1.548(3) | 1.548(3) | 1.588(2) | 1.587(3) | 1.592(3) |
| P2–N1 | 1.585(3) | 1.576(3) | 1.596(3) | 1.589(3) | 1.585(4) |
| P2–N2 | 1.548(3) | 1.549(3) | 1.603(3) | 1.601(3) | 1.591(4) |
| P3–N2 | 1.614(3) | 1.613(3) | 1.587(3) | 1.589(2) | 1.591(3) |
| P3–N3 | 1.613(3) | 1.619(3) | 1.598(3) | 1.600(3) | 1.599(4) |
| P3–N4 | 1.606(3) | 1.628(2) | 1.666(3) | 1.668(3) | 1.647(3) |
| P3–N5 | 1.632(3) | 1.633(2) | 1.664(2) | 1.679(3) | 1.657(3) |
| N1–P1–N3 | 120.56(16) | 120.69(14) | 116.10(13) | 115.67(14) | 116.28(18) |
| N8–P1–N9 | | | 101.69(14) | 100.76(14) | 100.37(19) |
| N1–P2–N2 | 119.83(17) | 119.70(15) | 116.99(13) | 117.99(13) | 116.32(19) |
| N6–P2–N7 | | | 103.14(14) | 104.72(13) | 100.31(19) |
| N2–P3–N3 | 113.14(15) | 113.09(13) | 117.66(13) | 117.73(13) | 114.96(18) |
| N5–P3–N4 | 102.68(16) | 103.14(13) | 102.16(13) | 101.86(13) | 98.94(17) |
| P1–N1–P2 | 118.50(19) | 118.74(18) | 123.50(16) | 122.64(16) | 112.8(2) |
| P3–N2–P2 | 124.1(2) | 124.34(16) | 121.72(16) | 120.54(15) | 124.0(2) |
| P1–N3–P3 | 123.34(18) | 123.22(17) | 122.68(15) | 123.53(15) | 123.9(2) |

The solvent was evaporated completely, and the oily residue was chromatographed [silica gel, eluent dichloromethane–THF (7:1)]. Two isomeric compounds were isolated. The first one was the cis isomer (**21a**; THF, $R_f = 0.76$). Yield: 0.28 g (48%). Mp: 231–232 °C. Anal. Calcd for $C_{32}H_{44}N_7O_2Fe_2P_3$: C, 50.35; H, 5.81; N, 12.84. Found: C, 50.84; H, 6.03; N, 12.57. APIES-MS (fragments are based on ^{56}Fe , Ir %): m/z 763 ($[M]^+$, 6.9). FTIR (KBr, cm^{-1}): ν 3373, 3280 (N–H), 3076, 3094 (C–H aromatic), 2932, 2846 (C–H aliphatic), 1234, 1178 (P=N). 1H NMR (500 MHz, $CDCl_3$, ppm; numbering of H atoms is given in Scheme 1): δ 4.45 (m, 4H, OCH_2), 4.27 (m, 4H, H2), 4.12 (m, 10H, H4), 4.18 and 3.86 (m, 2H, H5), 4.08 (m, 4H, H3), 3.35 (m, 4H, $NHCH_2$), 3.17 and 2.88 (m, 4H, NCH_2), 2.41 (bp, 2H, NH), 1.83 (m, 4H, NCH_2CH_2), 1.40 (m, 4H, OCH_2CH_2). ^{13}C NMR (500 MHz, $CDCl_3$, ppm; numbering of C atoms is given in Scheme 1): δ 86.81 (s, C1), 69.74 and 69.59 (s, C2), 68.40 (s, C4), 67.72 and 67.57 (s, C3), 66.50 (s, OCH_2), 46.21 (d, $^2J_{PC} = 6.9$ Hz, C5), 44.60 (d, $^2J_{PC} = 5.8$ Hz, NCH_2), 41.25 (s, $NHCH_2$), 27.03 (s, NCH_2CH_2), 26.33 (s, OCH_2CH_2).

The second one was the trans compound (**21b**; THF, $R_f = 0.69$). Yield: 0.31 g (31%). Mp: 152–154 °C. Anal. Calcd for $C_{32}H_{44}N_7O_2Fe_2P_3$: C, 50.35; H, 5.81; N, 12.84. Found: C, 50.62; H, 5.96; N, 12.42. APIES-MS (fragments are based on ^{56}Fe , Ir %): m/z 764 ($[MH]^+$, 8.4). FTIR (KBr, cm^{-1}): ν 3373, 3228 (N–H), 3094, 3076 (C–H aromatic), 2932, 2870 (C–H aliphatic), 1234, 1178 (P=N). 1H NMR (500 MHz, $CDCl_3$, ppm; numbering of H atoms is given in Scheme 1): δ 4.57 (m, 4H, OCH_2), 4.32 and 4.25 (m, 4H, H2), 4.11 (m, 10H, H4), 4.20 and 3.93 (m, 2H, H5), 4.07 (m, 4H, H3), 3.52 and 3.28 (m, 4H, $NHCH_2$), 3.12 and 2.94 (m, 4H, NCH_2), 2.47 (bp, 2H, NH), 1.76 and 1.73 (m, 4H, NCH_2CH_2), 1.39 (m, 4H, OCH_2CH_2). ^{13}C NMR (500 MHz, $CDCl_3$, ppm; numbering of C atoms is given in Scheme 1): δ 85.74 (d, $^3J_{PC} = 1.8$ Hz, C1), 85.37 (d, $^3J_{PC} = 3.4$ Hz, C1), 69.89 and 69.75 (s, C2), 68.52 and 68.47 (s, C4), 69.44 and 69.38 (s, C3), 68.15 (d, $^2J_{PC} = 4.6$ Hz, OCH_2), 67.43 (d, $^2J_{PC} = 7.2$ Hz, OCH_2), 46.46 (d, $^2J_{PC} = 6.9$ Hz, C5), 46.02 (d, $^2J_{PC} = 7.3$ Hz, C5), 44.92 (d, $^2J_{PC} = 6.4$ Hz, NCH_2), 44.18 (d, $^2J_{PC} = 6.5$ Hz, NCH_2), 41.20 (d, $^2J_{PC} = 3.3$ Hz, $NHCH_2$), 26.83 and 26.60 (s, NCH_2CH_2), 25.90 (d, $^3J_{PC} = 6.3$ Hz, OCH_2CH_2).

X-ray Crystal Structure Determinations. The orange crystals of compounds **7**, **10**, **11**, and **15** were crystallized from *n*-heptane at room temperature. The selected bond lengths and angles are given in Table 1, crystallographic data are listed in Table 2, and hydrogen-bond data are given in the Supporting Information (Table S3). Crystallographic data were recorded on an

Table 2. Crystallographic Details

| | 7 | 10 | 11^a | 15 |
|---|----------------------------|------------------------------|------------------------|--------------------------|
| empirical formula | $C_{15}H_{20}Cl_4FeN_3P_3$ | $C_{26}H_{30}Cl_4Fe_2N_3P_3$ | $C_{30}H_{50}FeN_9P_3$ | $C_{42}H_{62}Fe_2N_9P_3$ |
| fw | 560.92 | 758.96 | 685.55 | 897.63 |
| cryst syst | orthorhombic | triclinic | triclinic | triclinic |
| space group | <i>Pbca</i> | $P\bar{1}$ | <i>P1</i> | <i>P1</i> |
| <i>a</i> (Å) | 11.8340(2) | 10.7820(2) | 13.4740(2) | 11.494(4) |
| <i>b</i> (Å) | 24.1107(4) | 11.5467(4) | 15.0389(3) | 15.259(3) |
| <i>c</i> (Å) | 16.0267(3) | 13.2829(4) | 19.6478(5) | 15.293(3) |
| α (deg) | 90.00 | 68.19(2) | 68.54(3) | 60.98(2) |
| β (deg) | 90.00 | 79.75(2) | 87.08(3) | 75.49(2) |
| γ (deg) | 90.00 | 88.62(3) | 66.311(15) | 71.33(2) |
| <i>V</i> (Å ³) | 4572.83(14) | 1509.2(3) | 3371.5(9) | 2207.4(1) |
| <i>Z</i> | 8 | 2 | 4 | 2 |
| μ (cm ⁻¹) | 1.350 | 1.502 | 0.625 | 0.807 |
| ρ_{calcd} (g cm ⁻³) | 1.630 | 1.670 | 1.349 | 1.351 |
| no. of total reflns | 4628 | 6368 | 14082 | 9389 |
| no. of unique reflns | 4628 | 6092 | 13668 | 8924 |
| R_{int} | 0.0000 | 0.0178 | 0.0158 | 0.0435 |
| $2\theta_{\text{max}}$ (deg) | 52.60 | 52.58 | 52.58 | 52.58 |
| $T_{\text{min}}/T_{\text{max}}$ | 0.6452/ 0.8157 | 0.6400/ 0.7981 | 0.829/ 0.911 | 0.6696/ 0.7536 |
| no. of param | 257 | 361 | 775 | 505 |
| $R [F^2 > 2\sigma(F^2)]$ | 0.0438 | 0.0412 | 0.0480 | 0.0602 |
| w <i>R</i> | 0.1094 | 0.1060 | 0.1244 | 0.1567 |

^a The crystallographic data for compound **11** do not sufficiently fulfill the requirements of the checkCIF program, but the data of **11** were used in this study for comparison with the data (bond lengths and angles, hydrogen bondings, and conformation of the rings and Cremer–Pople parameters) of **7**, **10**, and **15**.

Enraf-Nonius CAD-4 diffractometer using Mo $K\alpha$ radiation ($\lambda = 0.71073$ Å) at $T = 294(2)$ K. Absorption corrections by ψ scan²⁹ were applied. Structures were solved by direct methods and refined by full-matrix least squares against F^2 using all data.³⁰ All non-H atoms were refined anisotropically. In compound **7**, only the H atom of the NH group was located in a difference synthesis and refined isotropically [$N-H = 0.875(19)$ Å; $U_{\text{iso}}(H) = 0.063(4)$ Å²]. The remaining H-atom positions were calculated geometrically at distances of 0.93 and 0.98 Å (CH) and 0.97 Å (CH₂) from the parent C atoms; a riding model was used during the refinement process, and the $U_{\text{iso}}(H)$ values were constrained to be $1.2U_{\text{eq}}$ (carrier atom).

Results and Discussion

Synthesis. The starting mono- and bisferrocenyldiamines (**1–5**) have been obtained from the reactions of ferrocenecarboxaldehyde and appropriate diamines, according to the published procedures.²⁸ The reactions of $N_3P_3Cl_6$ with mono- (**1** and **2**) and bisferrocenyl diamines (**3–5**) produce spirocyclic mono- (**6** and **7**) and bisferrocenylphosphazene (**8–10**) skeletons, respectively. Scheme 1 depicts tentatively the reaction pathway of $N_3P_3Cl_6$ with the ligands for providing a better understanding of the nucleophilic replacement reactions. The reactions of $N_3P_3Cl_6$ with the diamines (**1–5**) appear to be regioselective because the spiro arrangement is only favored, in contrast to other possibilities, such as ansa and bino products. Compounds **6–10** are the first examples of a spiro structure having ferrocenyldiamino

(29) North, A. C. T.; Phillips, D. C.; Mathews, F. S. *Acta Crystallogr., Sect. A* **1968**, *24*, 351–359.

(30) Sheldrick, G. M. *SHELXS-97*; University of Göttingen: Göttingen, Germany, 1997.

Table 3. Expected Geometrical and Optical Isomers for Compounds 16–21

| Compound | Stereogenic P-atoms (n) | Enantiomers | Enantiomer numbers, (2) ⁿ | Isomer numbers |
|----------|-------------------------|---|--------------------------------------|----------------------|
| 16 | 1 | R and S | 2 | |
| 17 | 2 | e2 $\left[\begin{array}{l} RR \\ RS \\ SR \\ SS \end{array} \right]$ e1 | 4 | |
| 18 | 3 | e2 $\left[\begin{array}{l} RRR \\ SRR \\ SSR \\ SSS \end{array} \right]$ e1 e4 $\left[\begin{array}{l} RSR \\ RRS \\ SRS \end{array} \right]$ e3 | 8 | 4 (cis) 4 (trans) |
| 19 | 3 | e2 $\left[\begin{array}{l} RRR \\ SRR \\ SSR \\ SSS \end{array} \right]$ e1 e4 $\left[\begin{array}{l} RSR \\ RRS \\ SRS \end{array} \right]$ e3 | 8 | 4 (cis) 4 (trans) |
| 20 | 2 | e2 $\left[\begin{array}{l} RR \\ RS \\ SR \\ SS \end{array} \right]$ e1 (meso) | 4 | 1 (cis) 2 (trans) |
| 21 | 2 | e2 $\left[\begin{array}{l} RR \\ RS \\ SR \\ SS \end{array} \right]$ e1 (Meso) | 4 | 1 (cis) 2 (trans) |

↔ enantiomers (e)
— diastereoisomers

The schematic representations of optical isomers for 17–21.

precursors. The tetrapyrrolidinophosphazenes (**11–15**) have been prepared by the reactions of corresponding partly substituted phosphazenes (**6–10**) with excess pyrrolidine in boiling THF. The possible ligating agents **16** and **17** for alkali and alkaline-earth metal cations have been obtained from the reactions of **6** with 1-aza-12-crown-4 in boiling *o*-xylene. Interestingly, the ³¹P NMR spectrum of **16** indicates that it has a geminal structure. This is very important evidence for the reaction pathway of **6** with 1-aza-12-crown-4 (Scheme 1). In addition, the partly substituted ferrocenylphosphazenes (**6**, **7**, **9** and **10**) give bis(N/O)-spiroposphazene skeletons (**18–21**) with sodium (3-amino-1-propanoxide) in boiling THF.

Table 3 outlines the geometrical and optical isomers of compounds **16–21**. The cis (**18a–21a**) and trans (**18b–21b**) isomers are separated from the mixtures by column chromatography (Figure 1), and the *R_f* values (see the experimental part) of the cis isomers are larger than those of the trans ones. No effort has been made to separate the optical isomers, while the presence of the

optically active species has been observed by the addition of CSA (Figures 1 and 2).

The microanalysis, FTIR, APIES-MS, and NMR data are consistent with the proposed structures of the compounds. While the mass spectra of **7**, **10–15**, and **21a** and **6**, **8**, **9**, **16**, **18a**, **18b**, **19a**, **19b**, **20b**, and **21b** show the molecular (*M*⁺) and protonated molecular ion (*MH*⁺) peaks, respectively, in the spectra of **17** and **20a**, the *M*⁺ peaks do not appear, but important fragments are observed at *m/z* 824 [*M* – (C₅H₁₁O₂ + Cl)]⁺ for **17** and at 566 [*MH* – Fc]⁺ for **20a**.

IR and NMR Spectroscopy. The FTIR spectra of all of the spirocyclic mono- and bisferrocenylphosphazenes display strong stretching bands between 1244 and 1176 cm⁻¹ attributed to *ν*_{P=N} bonds of the phosphazene ring.^{2c,20a} Asymmetric and symmetric stretching vibrations of *ν*_{Ar-H} are observed at 3096–3084 and 3078–3070 cm⁻¹. As expected, two kinds of *ν*_{PCl₂} absorption peaks, namely, asymmetric and symmetric vibrations have arisen for the tetrachloro derivatives (**6–10**) in the

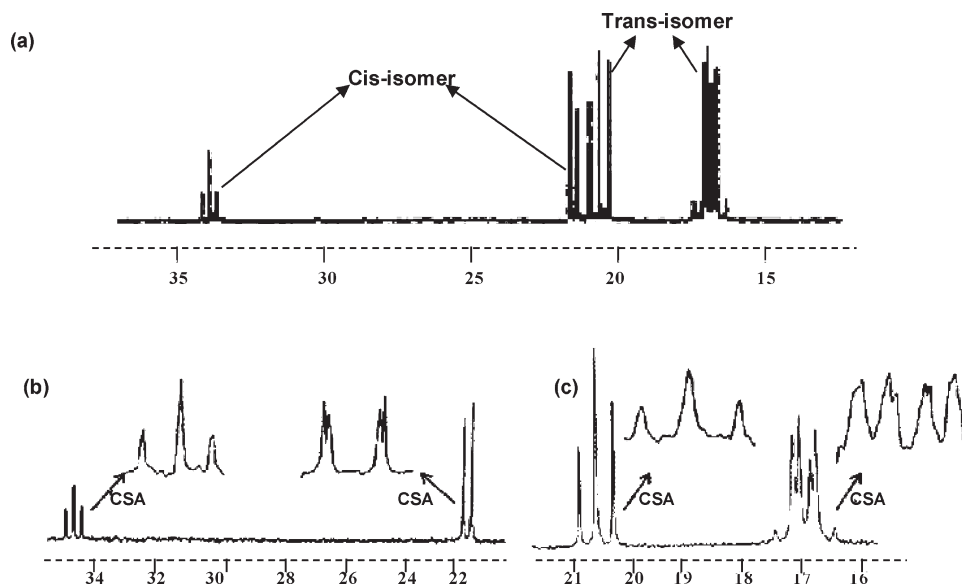


Figure 1. (a) ^{31}P NMR spectrum of a mixture of cis and trans isomers of **19**. (b) ^{31}P NMR spectrum of the cis isomer (**19a**) before the addition of CSA and after the addition of 10 drops of CSA. (c) ^{31}P NMR spectrum of the trans isomer (**19b**) before the addition of CSA and after the addition of 10 drops of CSA.

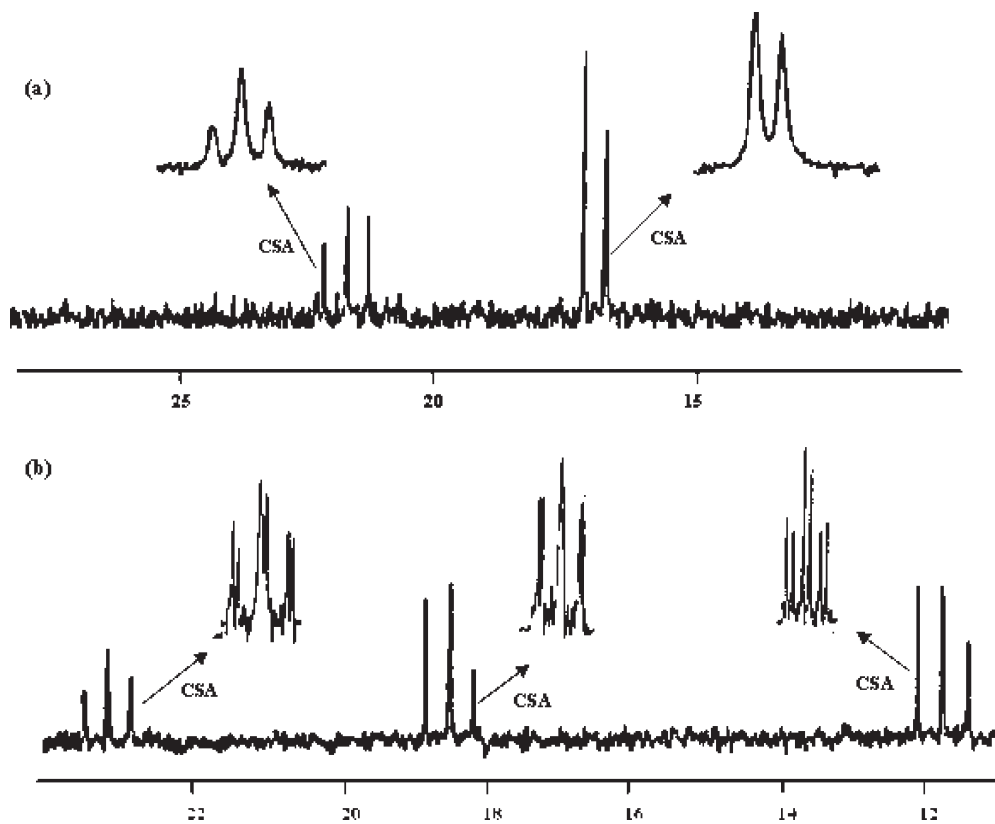


Figure 2. (a) ^{31}P NMR spectrum of the cis isomer (**21a**) before the addition of CSA and after the addition of 10 drops of CSA. (b) ^{31}P NMR spectrum of the trans isomer (**21b**) before the addition of CSA and after the addition of 10 drops of CSA.

ranges of 571–563 and 529–508 cm^{-1} . In the IR spectra of **6**, **7**, **10**, **11**, **12**, **15**, **19a**, **20a**, **21a**, and **18b–21b**, $\nu_{\text{N-H}}$, $\nu_{\text{CH}\cdots\text{N}}$, and/or $\nu_{\text{NH}\cdots\text{N}}$ (hydrogen-bond) stretching bands are observed between 3429 and 3308 cm^{-1} and between 3281 and 3202 cm^{-1} . The data obtained from the X-ray structural analyses of **7**, **10**, **11**, and **15** indicate the presence of intramolecular C–H \cdots N for **7**, **10**, **11**, and **15** and intermolecular N–H \cdots N for **7** hydrogen bonds (Supporting Information, Table S3).

The ^1H -decoupled ^{31}P NMR data of the phosphazenes are listed in Table 4. The data indicate that all of the compounds have spiro architectures. The spin systems are interpreted as AX₂, AB₂, ABX, AMX, and ABC (Table 4). Figure 3 depicts the spatial view of the compounds **6–21** for better understanding. Compounds **6–15** show a typical five-line resonance pattern consisting of a triplet for one P(spiro) atom and a doublet for two other P atoms. As expected, compounds **16** and **17** show a

Table 4. ^{31}P NMR (Decoupled) Spectral Data of the Compounds [Chemical shifts (δ) Reported in ppm and J values in Hz]^a

$\text{R}_1 = \text{H}$ or Fc-CH_2

| compound | δ (ppm) | | | | $^2J_{\text{PP}}$ (Hz) |
|------------------------|----------------|--|---------------------------|--------------------------|------------------------|
| | PCl_2 | $\text{P}(\text{NR})_2$ | $\text{P}(\text{pyrr})_2$ | $\text{P}(\text{ORN})$ | |
| 6 | 21.73 (d) | 15.80 (t) | | | 40.0 |
| 7 | 21.00 (d) | 13.62 (t) | | | 45.4 |
| 8 | 23.73 (d) | 16.74 (t) | | | 41.4 |
| 9 | 21.95 (d) | 11.47 (t) | | | 36.5 |
| 10 | 20.35 (d) | 14.56 (t) | | | 43.7 |
| 11 | | 20.76 (t) | 18.90 (d) | | 36.0 |
| 12 | | 21.92 (t) | 19.05 (d) | | 39.8 |
| 13 | | 26.80 (t) | 18.44 (d) | | 41.6 |
| 14 | | 23.25 (t) | 18.23 (d) | | 34.5 |
| 15 | | 22.08 (t) | 18.21 (d) | | 44.0 |
| 16 | 21.56 (dd) | 14.80 (dd) 22.33 (dd) | | | 29.8 44.0 49.2 |
| 17 | | 14.84 (dd) (spiro) 21.49 (dd) [P(NR)Cl] 22.41 (dd) (PCl ₂) | | | 28.2 45.0 48.7 |
| 18a^b | | 18.30 | | 17.53 17.29 | |
| 18b^b | | 19.07 (dd) | | 17.25 (dd) 16.99 (dd) | |
| 19a | | 34.42 (t) | | 21.63 (d) | 43.4 |
| 19b | | 20.88 (dd) | | 17.13 (dd) 16.67 (dd) | 52.0 53.3 |
| 20a | | 21.34 (t) | | 17.88 (d) | 56.8 |
| 20b^b | | 21.39 (dd) | | 18.18 (dd) 17.91 (dd) | 44.6 |
| 21a | | 20.96 (t) | | 17.11 (d) | 54.2 |
| 21b | | 23.19 (dd) | | 11.77 (dd) 18.51 (dd) | 53.5 55.9 57.4 |

^a ^{31}P NMR measurements in CDCl_3 solutions at 293 K. ^b $^2J_{\text{PP}}$ values are not calculated because of the overlapping signals.

12-line resonance pattern consisting of a doublet of doublets for all of the P atoms. ^{31}P NMR of **16** indicates that it has a geminal structure (Figure 3a and Supporting Information, Figure S4). The cis isomers, **18a–21a**, give a doublet for PON P atoms and a triplet for P(spiro) atoms, whereas the trans isomers, **18b–21b**, give, separately, doublet of doublets for the three P atoms. Hence, cis and trans isomers are easily distinguishable. In other words, according to the signal patterns in the ^{31}P NMR spectra of **18–21**, it can easily be determined whether these phosphazenes prepared by the reaction of sodium (3-amino-1-propanoxide) with tetrachlorophosphazenes (**6**, **7**, **9**, and **10**) have cis (**18a–21a**) or trans (**18b–21b**) geometric isomers. Two P atoms in spirocyclic bisferrocenylphosphazene (**20** and **21**) and three P atoms in monoferrocenylphosphazene (**18** and **19**) are expected to be stereogenic P atoms. Compounds **20** and **21** are expected to exist as cis (**20a** and **21a**) and/or trans (**20b** and **21b**) geometric isomers and to be cis (meso)

and/or trans (racemic) mixtures (Table 3). On the other hand, compounds **18** and **19** may be enantiomeric mixtures, and they exist as cis (**18a** and **19a**) and trans (**18b** and **19b**) geometric isomers. Compound **17** also has two stereogenic P atoms, and it has to be in the mixture of enantiomers (Table 3). In order to establish the stereogenic properties of these compounds, the representative phosphazenes (**19a**, **19b**, **21a**, and **21b**) are chosen, and they have been examined by ^{31}P NMR spectroscopy upon the addition of CSA using the literature procedure.^{21a} The effect of the addition of CSA on ^{31}P NMR signals for **19a**, **19b**, **21a**, and **21b** is summarized in Table 5. In general, changes of the ^{31}P NMR chemical shifts (expressed in ppb) and the magnitudes of $^2J_{\text{PP}}$ coupling constants of compounds **19a**, **19b**, **21a**, and **21b** are observed because of complexation with CSA. As expected for a meso compound, there is no splitting of signals for the cis isomer (**21a**; Figure 2a) even upon the addition of CSA up to a molar ratio of 40:1.

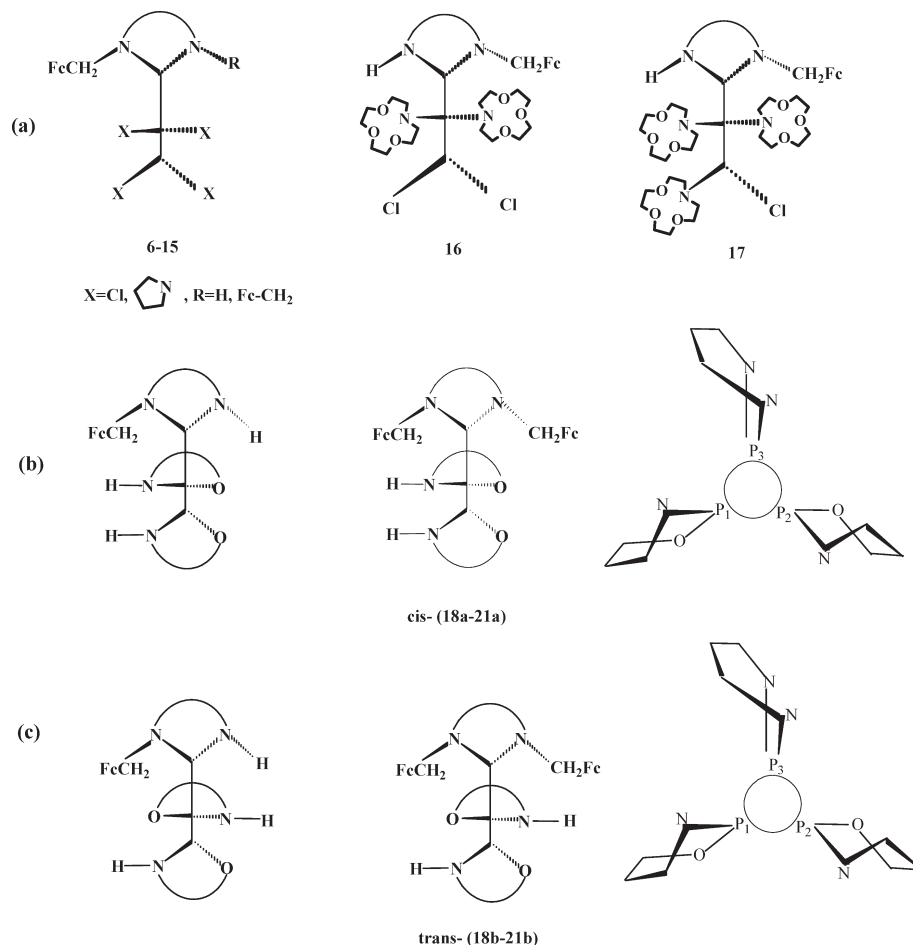


Figure 3. (a) Spatial views of **6–15**, **16**, and **17**. The possible geometric isomers and propeller views of (b) cis isomers (**18a–21a**) and (c) trans isomers (**18b–21b**).

However, the signals for the trans isomers (**21b**) split into two lines of equal intensity, indicating a racemate (Figure 2b). The P(ORN) signals of compounds **19a** (cis isomer) and **19b** (trans isomer) having three stereogenic P atoms split into two lines (Figure 1b,c) indicate that they exist as enantiomers (Table 3). In addition, the spiro P(NR)₂ signals of **19a** and **19b** are not clearly affected upon addition of CSA (Figure 1b,c). It is likely to depend on the weak complexation of the seven-membered precursors with CSA.

The coupling constants of all of the compounds are between 28.2 and 57.4 Hz.^{6a,9c} The magnitudes of ²J_{PP} are different for the cis (**18a–21a**) and trans (**18b–21b**) compounds (Table 4). Such differences in the NMR values of geometric isomers of cyclophosphazenes have been previously observed.^{24b,31}

In all of the spirophosphazene architectures, the ¹H and ¹³C NMR signals were assigned on the basis of chemical shifts, multiplicities, and coupling constants. Moreover, the assignments were made unambiguously by HETCOR, HMBC, COSY, and DEPT spectra (Supporting Information, Table S7). The spectra of **7** and **11** are depicted in the Supporting Information (Figures S5 and S6), as examples. All of the ¹H and ¹³C NMR assignments are written on the spectra.

The compounds **11–21** give complex ¹H NMR spectra. The spectra of mono- and bisferrocenyl trispirocyclic compounds (**18–21**) are especially highly complex because all of the aliphatic protons are diastereotopic. The protons of cyclopentadienyl rings are separated from each other and can easily be distinguished using HETCOR and HMBC (Supporting Information, Figure S5). The geminal FcCH₂N protons of **16**, **17**, **18b**, **19a**, **19b**, **20a**, **20b**, **21a**, and **21b** give rise to an ABX spin system because of the geminal proton–proton coupling and the vicinal coupling with the P-31 nucleus. The ³J_{PH} values of FcCH₂N protons are between 9.9 and 12.7 Hz for tetrachloro (**6–10**), 3.5–7.4 Hz for tetrapyrrolidino (**11–15**), and 7.4–11.2 Hz for trispirocyclic (**18–21**) phosphazene derivatives. This means that the ³J_{PH} values of tetrapyrrolidino derivatives are smaller than those of tetrachloro and trispirocyclic ones.

In the ¹H NMR spectra of monoferrocenyltetrapyrrolidinophosphazenes (**11** and **12**), the two pyrrolidino substituents bonded to the same P atom show two groups of NCH₂(pyrr) signals (3.10 and 3.25 ppm for **11** and 3.14 and 3.22 ppm for **12**) with small separations. As expected, the same situation is observed for NCH₂CH₂(pyrr) protons (Figure 3a).

All of the expected carbon peaks are interpreted from the ¹³C NMR spectra of the compounds. In the tetrachloro (**7** and **10**), tetrapyrrolidino (**12** and **15**), and trispirocyclic phosphazenes (**19a**, **19b**, **21a**, and **21b**)

(31) Krishnamurthy, S. S.; Woods, M. *Annu. Rep. NMR Spectrosc.* **1987**, *19*, 175–320.

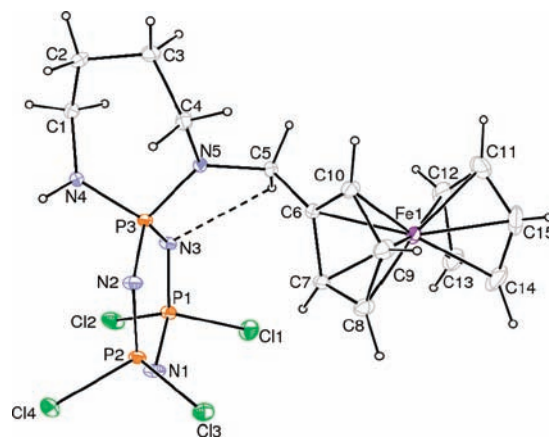
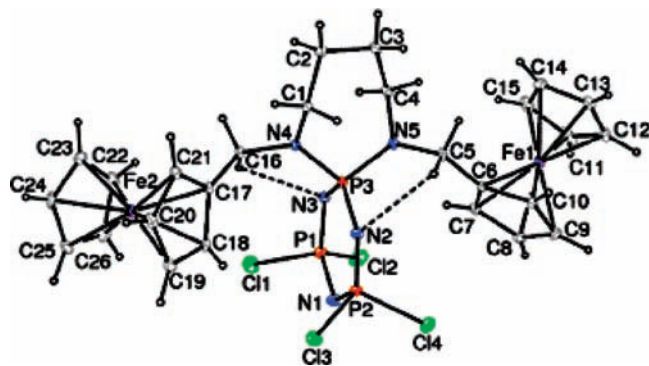
Table 5. ^{31}P NMR Parameters of Compounds **19a**, **19b**, **21a**, and **21b** and Effect of CSA on the ^{31}P NMR Chemical Shifts^a

| compound | chemical shift/ppm | | $^2J_{\text{PP}}/\text{Hz}$ |
|--|---------------------|------------|-----------------------------|
| | >P(NR) ₂ | >P(ORN) | |
| (i) Structural Assignment of Signals | | | |
| 19a | 34.42 (t) | 21.63 (d) | 43.4 |
| 19b | 20.88 (dd) | 16.67 (dd) | 52.0 |
| | | 17.13 (dd) | 53.3 |
| | | | 56.8 |
| 21a | 20.96 (t) | 17.11 (d) | 54.2 |
| 21b | 23.19 (dd) | 11.77 (dd) | 53.5 |
| | | 18.51 (dd) | 55.9 |
| | | | 57.4 |
| (ii) Effect of CSA on the ^{31}P NMR Chemical Shifts (ppb) at a 15:1 Mole Ratio | | | |
| 19a | 360 | 120 | 43.0 |
| 19b | -10 | -60 | 52.2 |
| | | -60 | 54.0 |
| | | | 55.6 |
| 21a | 60 | -90 | 53.8 |
| 21b | 260 | 340 | 53.1 |
| | | 340 | 56.6 |
| | | | 58.7 |
| (iii) Separation of Enantiomeric Signals (ppb) at a 15:1 Mole Ratio of CSA–Molecule | | | |
| 19a | b | 26 | |
| 19b | b | 25 | |
| | | 40 | |
| 21a^c | | | |
| 21b | 40 | 129 | |
| | | 37 | |

^a ^{31}P NMR measurements in CDCl_3 solutions at 293 K. ^b Magnitude of the effect too small to observe up to a 15:1 mole ratio. ^c As expected, no effect was observed up to a mole ratio of at least 40:1.

containing seven-membered spirorings, the signals of C1 are shifted downfield according to the six- (**6**, **9**, **11**, **14**, **16**, **17**, **18a**, **18b**, **20a**, and **20b**) and five-membered spirophosphazenes (**8** and **13**). The $\text{NCH}_2(\text{pyrr})$ and $\text{NCH}_2\text{CH}_2(\text{pyrr})$ signals of monoferrocenyltetrapyrrolidino-phosphazenes (**11** and **12**) are assigned by HETCOR and HMBC experiments (Supporting Information, Table S7). Two group peaks [$\delta(\text{NCH}_2) = 46.00$ and 46.30 ppm for **11**, $\delta(\text{NCH}_2) = 46.10$ and 46.32 ppm for **12**; $\delta(\text{NCH}_2\text{CH}_2) = 26.42$ and 26.46 ppm for **11**, and $\delta(\text{NCH}_2\text{CH}_2) = 26.38$ and 26.42 ppm for **12**] are also distinguishable for geminal pyrrolidine rings (Figure 3a).

The molecular structures of compounds **18–21** look like a propeller, where the spiro(3-amino-1-propanoxy) ring's orientation gives rise to the *cis* and *trans* isomers (Figure 3b,c). Hence, in the ^{13}C NMR spectra of *cis*-mono- (**19a**) and *cis* (meso)-bisferrocenylphosphazenes (**20a** and **21a**), each of the carbon signals has been observed as two signal sets for the C2 and C3 of ferrocene (Fc) C atoms. In the ^{13}C NMR spectrum of *trans*-phosphazene (**19b**), all of the C atoms give two different carbon signals, which appear to belong to diastereoisomers (Table 3), whereas in **18b**, which is also a *trans* compound, only C2 and C3 Fc C atoms are distinguishable. All of the carbon signals of *cis* (meso)-phosphazene (**20a**) are determined by using the HETCOR spectrum. The HETCOR experiments are also especially useful for determining the carbon signals of **16**

**Figure 4.** (a) ORTEP-3³⁷ drawing of **7** with the atom-numbering scheme. Displacement ellipsoids are drawn at the 30% probability level.**Figure 5.** (a) ORTEP-3³⁷ drawing of **10** with the atom-numbering scheme. Displacement ellipsoids are drawn at the 30% probability level.

and **17** with bis- and tris-crown ether units (Supporting Information, Table S7).

The three-bond couplings of **11**, **13**, **14**, **15**, **19a**, and **20a** (for pyrrolidine and 3-amino-1-propanoxy groups) give rise to triplets in the case of doublets, as depicted in the Supporting Information (Figure S7). The triplets observed for the pyrrolidine C atoms (NCH_2CH_2) (**11** and **13–15**) may be due to second-order effects, which have previously been observed.³² The $^3J_{\text{PC}}$ coupling constants between the external transitions of the triplets have been estimated.³³

As expected, the peaks of nonprotonated C atoms disappear in the DEPT spectra, as compared with the ^1H -decoupled ^{13}C NMR spectra. The spectrum of **11** is depicted in the Supporting Information (Figure S6), as an example.

X-ray Structures of 7, 10, 11, and 15. The X-ray structural determinations of compounds **7**, **10**, **11**, and **15** confirm the assignments of their structures from spectroscopic data. The asymmetric unit of **11** contains two crystallographically independent molecules. The molecular structures and packing diagrams of compounds **7**, **10**, **11**, and **15**, along with the atom-numbering schemes, are depicted in Figures 4–7, respectively. The phosphazene

(32) (a) Shaw, R. A. *Phosphorus, Sulfur, Silicon* **1989**, *45*, 103–136. (b) Bilge, S.; Özgüç, B.; Safran, S.; Demiriz, S.; İşler, H.; Hayvalı, M.; Kılıç, Z.; Hökelek, T. *J. Mol. Struct.* **2005**, *748*, 101–109.

(33) Vicente, V.; Fruchier, A.; Cristau, H. *J. Magn. Reson. Chem.* **2003**, *41*, 183–192.

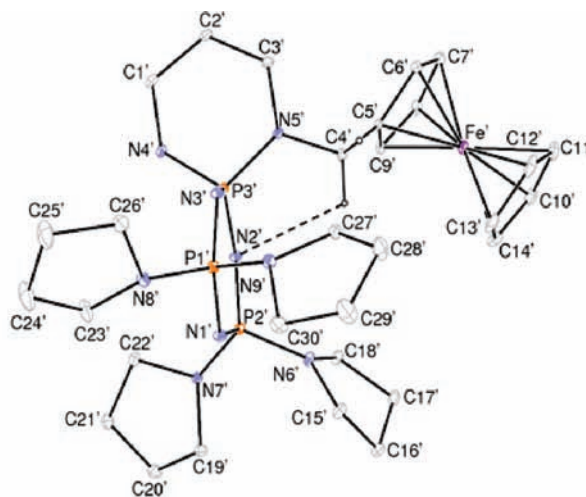
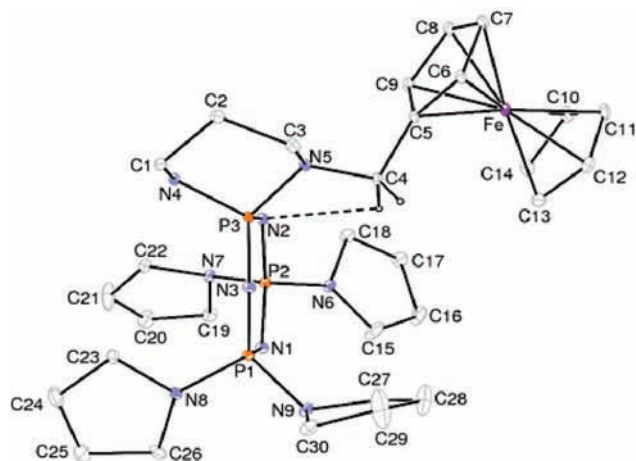


Figure 6. (a) ORTEP-3³⁷ drawing of **11** with the atom-numbering scheme. Displacement ellipsoids are drawn at the 30% probability level.

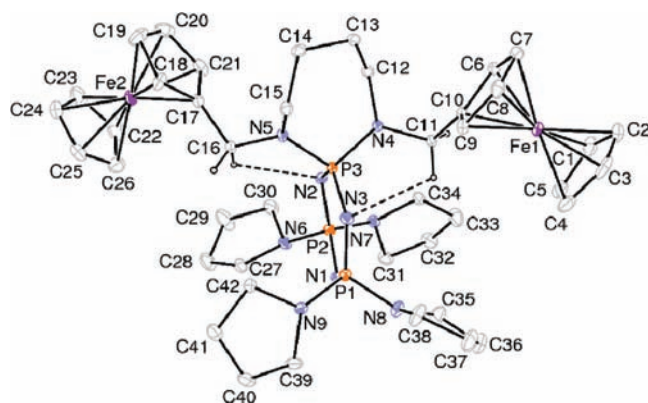


Figure 7. (a) ORTEP-3³⁷ drawing of **15** with the atom-numbering scheme. Displacement ellipsoids are drawn at the 30% probability level.

rings of **7** and **10** are nearly planar [Supporting Information, Figures S4b and S5b), while **11** and **15** are not planar but in flattened-boat forms [Supporting Information, Figure S6b, $\varphi_2 = -68.6(3.3)^\circ$, $\theta_2 = 26.1(1.4)^\circ$; Supporting Information, Figure S6b, $\varphi_2 = -89.3(1.0)^\circ$, $\theta_2 = 102.6(8)^\circ$; Supporting Information, Figure S7b, $\varphi_2 = 158.3(1.2)^\circ$, $\theta_2 = 87.1(0.5)^\circ$] having total puckering amplitudes Q_T of 0.075(2) (for **7**), 0.048(2) (for **10**), 0.098(2) and 0.151(3) (for **11**), and 0.287(5) (for **15**).³⁴

In **11**, the six-membered rings P3/N4/N5/C1–C3 and P3'/N4'/N5'/C1'–C3' are in chair conformations [Supporting Information, Figure S6c, $Q_T = 1.070(8) \text{ \AA}$, $\varphi_2 = -31.3(4)^\circ$, $\theta_2 = 117.9(2)^\circ$; Supporting Information, Figure S6c, $Q_T = 1.121(8) \text{ \AA}$, $\varphi_2 = -32.5(4)^\circ$, $\theta_2 = 117.7(2)^\circ$]. In **7**, the seven-membered ring P3/N4/N5/C1–C4 is in the twisted form [Supporting Information, Figure S4c, $Q_T = 1.308(5) \text{ \AA}$, $\varphi_2 = -46.7(2)^\circ$, $\varphi_3 = -157.2(3)^\circ$, and $\theta_2 = 50.4(2)^\circ$]. In **10** and **15**, the seven-membered rings P3/N4/N5/C1–C4 for **10** and P3/N4/N5/C12–C15 for **15** are also in twisted forms [Supporting Information, Figure

S5c, $Q_T = 1.348(5) \text{ \AA}$, $\varphi_2 = 130.1(2)^\circ$, $\varphi_3 = -23.4(3)^\circ$, and $\theta_2 = 50.1(1)^\circ$; Supporting Information, Figure S7c, $Q_T = 1.359(6) \text{ \AA}$, $\varphi_2 = 130.6(2)^\circ$, $\varphi_3 = -23.0(3)^\circ$, and $\theta_2 = 48.8(2)^\circ$].

The average P–N bond lengths in phosphazene rings are 1.582(3), 1.587(3), 1.594(3), and 1.593(4) Å, which are shorter than the average exocyclic P–N bonds of 1.619(3), 1.631(2), 1.659(3), and 1.652(3) Å for **7**, **10**, **11**, and **15**, respectively.

In the phosphazene rings, the endocyclic P–N bond lengths are in the ranges 1.548(3)–1.614(3) Å (for **7**), 1.548(3)–1.619(3) Å (for **10**), 1.587(3)–1.603(3) Å (for **11**), and 1.585(4)–1.599(4) Å (for **15**) and compounds **7** and **10** exhibit regular variations with the distances from P3: P3–N2 \approx P3–N3 > P2–N1 \approx P1–N1 > P1–N3 \approx P2–N2. On the other hand, the exocyclic P–N bonds for spirorings are P3–N4 [1.606(3) Å] and P3–N5 [1.632(3) Å] (for **7**), P3–N4 [1.628(2) Å] and P3–N5 [1.633(2) Å] (for **10**), P3–N4 [1.666(3) Å], P3–N5 [1.664(2) Å], P3'–N4' [1.668(3) Å], and P3'–N5' [1.679(3) Å] (for **11**), and P3–N4 [1.647(3) Å] and P3–N5 [1.657(3) Å] (for **15**) (Table 1). In phosphazenes, the PN single and double bonds are generally in the ranges of 1.628–1.691 and 1.571–1.604 Å, respectively,^{35a} and they are among the most intriguing bonds in chemistry. Recently, natural bond orbital (NBO) and topological electron density analyses were used to investigate the electronic structure of phosphazenes.^{35b} The most likely phosphazene bonding alternatives, namely, negative hyperconjugation and ionic bonding, are evaluated by using NBO. Ionic bonding was found to be the dominant feature, and the multiple-bond character could be attributed to the presence of negative hyperconjugation.^{35b,c}

As can be seen from Table 1, in **7**, **10**, and **15**, endocyclic N2–P3–N3 (α) angles are narrowed, while P3–N2–P2 (β) angles are expanded considerably with respect to the corresponding values in the “standard” compound, N₃P₃Cl₆. In N₃P₃Cl₆, the α and β angles are 118.3(2) and 121.4(3)°, respectively.³⁶ The variations in the angles found in phosphazenes could be attributed to the

(34) Cremer, D.; Pople, J. A. *J. Am. Chem. Soc.* **1975**, *97*(6), 1354–1358.

(35) (a) Allen, F. H.; Kennard, O.; Watson, D. G.; Brammer, L.; Orpen, G.; Taylor, R. *J. Chem. Soc., Perkin Trans. 2* **1987**, *12*, 1–19. (b) Chaplin, A. B.; Harrison, J. A.; Dyson, P. J. *Inorg. Chem.* **2005**, *44*, 8407–8417. (c) Krishnamurthy, S. S. *Phosphorus, Sulfur, Silicon Relat. Elem.* **1994**, *87*, 101–111.

(36) Bullen, G. J. *J. Chem. Soc. A* **1971**, 1450–1453.

(37) Farrugia, L. J. *J. Appl. Crystallogr.* **1997**, *30*, 565–566.

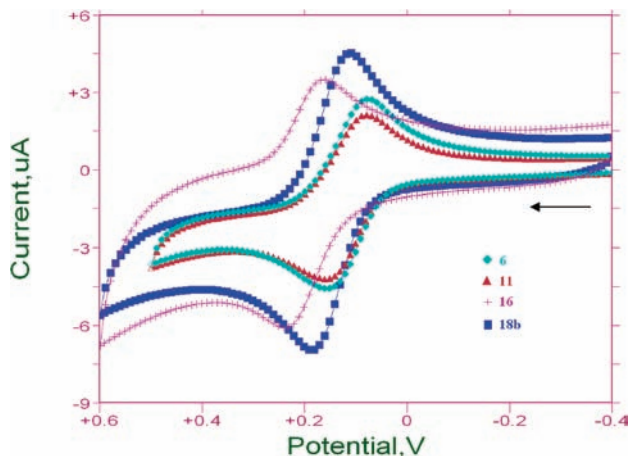


Figure 8. CVs of one-Fc-center phosphazene derivatives of **6**, **11**, **16**, and **18b** (1 mM each) in acetonitrile (0.1 M TBATFB) at a glassy carbon electrode versus Ag/AgCl/KCl_{sat}. The scan rate is 50 mV/s.

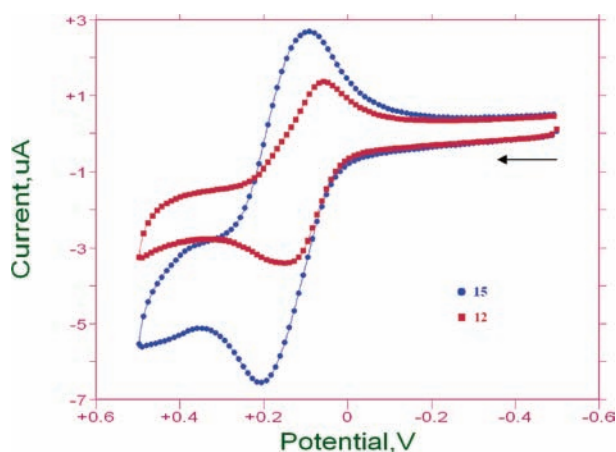


Figure 9. CVs of ferrocenylphosphazene derivatives (1 mM each) with one (**12**) and two (**15**) Fc centers in acetonitrile (0.1 M TBATFB) at the glassy carbon electrode versus Ag/AgCl/KCl_{sat}. The scan rate is 50 mV/s.

substituent-dependent charge at the P centers and negative hyperconjugation.^{35b}

Compounds **7**, **10**, **11**, and **15** have intramolecular Fc–CH–H···N hydrogen bonds (Figures 4–9). Compounds **7** and **11** have intermolecular N–H···N and C–H···N hydrogen bonds, respectively, linking phosphazene rings into chains (Supporting Information, Table S3 and Figures S8d and S10d). The $\pi\cdots\pi$ contacts between the five-membered ferrocene rings, Cg1---Cg2 (where Cg1 and Cg2 are centroids of the rings C6–C10 and C11–C15) with a centroid–centroid distance of 3.278(4) Å (for **7**), Cg1---Cg2 and Cg3---Cg4 [where Cg1, Cg2, Cg3, and Cg4 are centroids of the rings C6–C10, C11–C15, C17–C21, and C22–C26, respectively] with centroid–centroid distances of 3.285(2) and 3.286(3) Å (for **10**), Cg5---Cg6 and Cg7---Cg8 [where Cg5, Cg6, Cg7, and Cg8 are centroids of the rings C1–C5, C6–C10, C17–C21, and C22–C26, respectively] with centroid–centroid distances of 3.285(4) and 3.272(5) Å (for **15**), and Cg9---Cg11 and Cg10---Cg12 [where Cg9, Cg10, Cg11, and Cg12 are centroids of the rings C5–C9, C10–C14, C5'–C9', and C10'–C14', respectively] with centroid–centroid distances of 3.288(3) and 3.286(3) Å

(for **11**), may further stabilize the structure. There also exist C–H··· π interactions in compounds **10**, **11**, and **15** (Supporting Information, Table S3).

Electrochemistry of Ferrocenylphosphazenes. To investigate the electrochemical behaviors of ferrocenylphosphazenes and the effects of the structural differences on the electron-transfer kinetics, the cyclic voltammograms (CVs) of the compounds were acquired in acetonitrile (0.1 M TBATFB) at the glassy carbon electrode versus Ag/AgCl/KCl_{sat}. The electrochemical data of the compounds **6–21** are given in the Supporting Information (Table S8), and Figure 8 shows typical CVs of the phosphazenes containing different substituents in the phosphazene ring (chloro, pyrrolidino, crown ether, and N/O groups) with only one Fc group (**6**, **11**, **16**, and **18b**). At a first glance, it can be seen that all groups of compounds have reversible CVs with one-electron anodic and cathodic peaks corresponding to the redox-responsible moiety of the Fc substituent, which is a versatile redox probe. As shown in Figure 8, the shapes of the CV peaks are not significantly influenced by the structural changes in the phosphazene ring. The substitutions of pyrrolidine groups (**11** and **12**) with the chloride (**6** and **7**), N/O (**18b** and **19a**), and crown ether (**16** and **17**) groups in the phosphazene ring (for one Fc site) shift the redox potentials to more anodic values, suggesting that the Fc sites become more positive and difficult to oxidize, in the stated order. The presence of the crown ether groups results in significant shifts in the oxidation peak potentials of about 67 mV toward anodic values relative to the pyrrolidine-substituted derivatives.

Inspection of Table S8 (see Supporting Information) shows that the two Fc redox centers in the same molecule undergo oxidation concurrently at the same potential, which is an important property to act as a mediator. The length of the diamine alkyl chain [(CH₂)_n, where $n = 0, 1$, and 2] has no significant effect on the redox potential of the compounds, as can be understood if one compares the redox potentials for **6–7**; **8–10**; **11–12**; **13–15**; and **18b–19a**. The compounds **8–10**, **13–15**, **20b**, and **21a** all contain two Fc redox centers and exhibit only one CV wave with two-electron transfer, as compared to the ones containing one Fc redox center. The striking effects of the presence of two pendant Fc groups, although they are isolated from the phosphazene ring, make the Fc groups difficult to oxidize, which is apparent from the more positive redox potentials of these compounds.³⁸ Redox potentials are taken approximately equal to the half-wave potentials, assuming reversible oxidation and identical diffusion coefficients of the oxidized and reduced forms of ferrocenylphosphazenes. As Table S8 (column 2) (see the Supporting Information) shows, the redox potentials of two pendant Fc groups bearing chlorophosphazene derivatives of **8–10** and pyrrolidinophosphazene derivatives of **13–15** are more positive than that of one-Fc-bearing counterparts, which are **6–7** and **11–12**, respectively. The same behavior is true for N/O-bearing phosphazene derivatives. For example, the redox potentials of **18b** and **20b** are 157 and 216 mV, respectively; insertion of one Fc group

(38) Bard, A. J.; Faulkner, L. R. *Electrochemical Methods: Fundamentals and Applications*; John Wiley and Sons, Inc.: New York, 2001; p 230.

Table 6. Susceptibility Results of Compounds for Reference Strain: *M. tuberculosis* H37Rv^a

| compound | dilution rates and susceptibility results | | | | |
|-----------|---|----------|----------|----------|----------|
| | 10000 (S) | 5000 (S) | 2500 (S) | 1250 (S) | 1000 (S) |
| 11 | 10000 (S) | 5000 (S) | 2500 (S) | 1250 (S) | 1000 (S) |
| 12 | 10000 (S) | 5000 (S) | 2500 (S) | 1250 (S) | 1000 (S) |
| 14 | 10000 (S) | 5000 (S) | 2500 (S) | 1250 (S) | 1000 (S) |
| 15 | 10000 (S) | 5000 (S) | 2500 (S) | 1250 (S) | 1000 (S) |
| dioxan | 60% (R) | 30% (R) | | | |

^aR = resistant. S = sensitive.

results in an approximate 60 mV shift to the positive potentials.³⁹ Another important result that comes from the CVs is the number of electrons transferred for the compounds having one and two Fc centers. Figure 9 shows the CVs of pyrrolidino derivatives **12** and **15** for the same concentration and electrode area. The anodic peaks are calculated as 2.89 and 5.91 μA , corresponding to one- and two-electron transfers. The values of the currents clearly confirm that both ferrocenes are involved in the oxidation peaks of the pyrrolidino compounds that contain two Fc groups. Similar behavior has been reported by Gong et al. for the one-, two-, and three-Fc-branched ferrocenes.³⁹ The slopes of the anodic peak currents versus the square root of the scan rate also support this fact, as these values are 0.57 and 0.96 $\mu\text{A}/\text{mV}^{1/2}$ for **12** and **15**, respectively, assuming the diffusion coefficients are identical. The values of cathodic-to-anodic peak current ratios are very close to 1 for all compounds, indicating that there are no solubility differences between compounds and their oxidized forms^{9d} and the high electron-transfer rate of Fc centers.³⁸ The values of the slope of the $\log i_{\text{pa}}$ vs $\log \nu$ plots, being about 0.5, also verify that CVs are not influenced much because of the adsorption of either the compounds or their oxidized forms.

Susceptibility Testing: *M. tuberculosis* H37Rv. *M. tuberculosis* H37Rv reference strain is used for susceptibility testing. It is susceptible to serial dilutions of compounds **11**, **12**, **14**, and **15** and is resistant to 30% or 60% dioxan. The susceptibility results of compounds for reference strain are given in Table 6.

Conclusions

The phosphazene derivatives (**6–10**) are the first examples of a spiro structure having ferrocenyldiamino precursors. The fully substituted phosphazenes (**11–15** and **18–21**) are

prepared from the reactions of compounds **6–10** with pyrrolidine and sodium (3-amino-1-propanoxide). The possible ligating agents **16** and **17** for alkali and alkaline-earth metal cations are obtained from the reactions of **6** with 1-aza-12-crown-4. The stereogenic properties of the representative phosphazenes (**19a**, **19b**, **21a**, and **21b**) are determined by ³¹P NMR spectroscopy upon addition of CSA. The solid-state structures of **7**, **10**, **11**, and **15** reveal the strong intramolecular C–H···N and intermolecular N–H···N hydrogen bonding. In addition, all of the new phosphazenes, possessing electrochemically active groups, can be thought of as good candidates for electron-transfer mediators and materials for electronic devices. The electrochemical behavior of bisferrocenylphosphazenes indicates that all of them show a single reversible oxidation wave, suggesting the electrochemical equivalence of the pendant Fc groups. Compounds **11–15** have been evaluated in terms of antimicrobial activities against some Gram positive and Gram negative bacteria. All compounds have potential antibacterial activities against *Bacillus cereus*, which is Gram positive bacterium. Compound **11** also has very strong antifungal activity against *Candida albicans*. The compounds **11**, **12**, **14**, and **15** are evaluated for antituberculosis activity against reference strain *M. tuberculosis* H37Rv (ATCC 27294). In addition, compounds **11–15** are found to differ in their ability to cause the unwinding of supercoiled form I pBR322 plasmid DNA. All of the compounds are effective in changing the mobility of the pBR322 plasmid DNA; however, compound **12** has a stronger effect on form II plasmid DNA, and **13** has a different effect on plasmid supercoiled DNA than the other compounds.

Acknowledgment. The authors acknowledge the “Scientific and Technical Research Council of Turkey” (Grants 108T892 and 106T622). T.H. is indebted to “Hacettepe University, Scientific Researchs Unit” (Grant 02 02 602 002) for financial support.

Supporting Information Available: Additional figures giving crystal packing diagrams (**4d–7d**) and ring conformations (**4b–7b** and **4c–7c**), X-ray crystallographic files in CIF format for compounds **7**, **10**, **11**, and **15**, hydrogen-bond geometries (Table S3), 2D ¹H–¹³C HETCOR and HMBC correlations for compounds **7**, **11**, and **20a** (Table S7), CV data of ferrocenylphosphazene derivatives (Table S8), ¹H-coupled and ¹H-decoupled ³¹P NMR spectra of **16** (Figure S4), HETCOR, COSY, and HMBC spectra of **7** (Figure S5), ¹³C NMR and DEPT spectra of **11** (Figure S6), second-order effects in ¹³C NMR spectra of **13–15** and **19a** (Figure S7), antimicrobial activities (section S1), susceptibility testing of *M. tuberculosis* (section S2), and DNA and compound interactions (section S3). This material is available free of charge via the Internet at <http://pubs.acs.org>.

(39) Gong, Y.; Audebert, P.; Yang, F.; Miomandre, F.; Lian, X.; Tang, J. *J. Electroanal. Chem.* **2007**, *606*, 8–16.